

**AD-A278 560**



**PL-TR-93-2169**

(2)

**DEVELOPMENT OF A PRELIMINARY SOLAR  
WIND TRANSPORT MAGNETOSHEATH  
FORECAST MODEL**

**Stephen S. Stahara  
Richard R. Rachiele  
Gregory A. Molvik  
John R. Spreiter**

**RMA Aerospace, Inc  
883 North Shoreline Blvd  
Suite B200  
Mountain View, CA 94043**

**DTIC  
ELECTE  
MAR 22 1994  
S F D**

**July 1993**

**Final Report  
Period Covered: 11/91 - 7/93**

**94-09002**



**Approved for public release; distribution unlimited**




**PHILLIPS LABORATORY  
Directorate of Geophysics  
AIR FORCE MATERIEL COMMAND  
HANSCOM AIR FORCE BASE, MA 01731-3010**

**94 3 21 054**

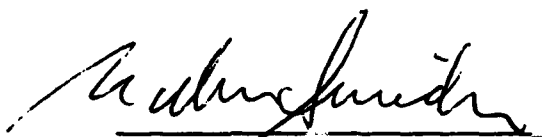
This technical report has been reviewed and is approved for publication.



MICHAEL A. HEINEMANN  
Contract Manager  
Space Plasmas and Fields Branch  
Space Physics Division



DAVID A. HARDY, Chief  
Space Plasmas and Fields Branch  
Space Physics Division



WILLIAM SWIDER  
Deputy Director  
Space Physics Division

This report has been reviewed by the ESC Public Affairs Office (PA) and is releasable to the National Technical Information Service (NTIS).

Qualified requestors may obtain additional copies from the Defense Technical Information Center. All others should apply to the National Technical Information Service.

If your address has changed, or if you wish to be removed from the mailing list, or if the addressee is no longer employed by your organization, please notify PL/TSI, Hanscom AFB, MA 01731-3010. This will assist us in maintaining a current mailing list.

Do not return copies of this report unless contractual obligations or notices on a specific document require that it be returned.

REPORT DOCUMENTATION PAGE			Form Approved OMB No. 0704-0188	
<small>Public reporting burden for this collection of information is estimated to average 1 hour per response, including the time for reviewing instructions, searching existing data sources, gathering and maintaining the data needed, and completing and reviewing the collection of information. Send comments regarding this burden estimate or any other aspect of this collection of information, including suggestions for reducing this burden, to Washington Headquarters Services, Directorate for Information Operations and Reports, 1215 Jefferson Davis Highway, Suite 1204, Arlington, VA 22202-4302, and to the Office of Management and Budget, Paperwork Reduction Project (0704-0188), Washington, DC 20503.</small>				
1. AGENCY USE ONLY (Leave blank)		2. REPORT DATE July 1993	3. REPORT TYPE AND DATES COVERED Final Nov 1991 - July 1993	
4. TITLE AND SUBTITLE  Development of a Preliminary Solar Wind Transport Magnetosheath Forecast Model			5. FUNDING NUMBERS  PE 63707F PR 2688 TA 04 WU KB F19628-90-C-0054	
6. AUTHOR(S)  Stephen S. Stahara Richard R. Rachiele			Gregory A. Molvik John R. Spreiter	
7. PERFORMING ORGANIZATION NAME(S) AND ADDRESS(ES)  RMA Aerospace, Inc. 883 North Shoreline Blvd Suite B200 Mountain View, CA 94043			8. PERFORMING ORGANIZATION REPORT NUMBER	
9. SPONSORING/MONITORING AGENCY NAME(S) AND ADDRESS(ES)  Phillips Laboratory 29 Randolph Road Hanscom AFB, MA 01731-3010 Contract Manager: Michael Heinemann/GPSG			10. SPONSORING/MONITORING AGENCY REPORT NUMBER  PL-TR-93-2169	
11. SUPPLEMENTARY NOTES				
12a. DISTRIBUTION/AVAILABILITY STATEMENT  Approved for public release; distribution unlimited			12b. DISTRIBUTION CODE	
13. ABSTRACT (Maximum 200 words)  An account is provided of the technical work carried out on the development of a preliminary solar wind transport magnetosheath forecast model during the period between delivery of the Phase I SWT model in November 1991 and the early termination of the contract in July 1993. The technical work during this period focused on validation of the SWT model and involved two primary technical tasks: (1) creation of the observational satellite data base against which the model was to be validated, and (2) initial comparative testing of the Phase I SWT model forecasts against these observations. Details of the results obtained from these two technical tasks are discussed. At the present stage of development, the SWT forecast model remains unqualified for operational use. An outline is provided of the technical tasks required to complete the qualification program.				
14. SUBJECT TERMS  Magnetosheath forecasts; real-time solar wind input; observational comparisons			15. NUMBER OF PAGES 46	
			16. PRICE CODE	
17. SECURITY CLASSIFICATION OF REPORT Unclassified	18. SECURITY CLASSIFICATION OF THIS PAGE Unclassified	19. SECURITY CLASSIFICATION OF ABSTRACT Unclassified	20. LIMITATION OF ABSTRACT SAR	

# TABLE OF CONTENTS

	PAGE
EXECUTIVE SUMMARY	vii
1. OVERVIEW OF SOLAR WIND TRANSPORT MAGNETOSHEATH FORECAST MODEL	1
1.1 Overall Objectives	1
1.2 Operational Elements of SWT Model	2
2. SATELLITE DATA BASE FOR VALIDATION OF SWT FORECAST MODEL	6
3. SWT MODEL VALIDATION PROGRAM	8
3.1 Previous Validation of Elements of the SWT model	8
3.2 Current Validation Results of the SWT Model	12
4. CONCLUSIONS AND RECOMMENDATIONS	13
4.1 Status of SWT Validation Program	13
4.2 Final Qualification of SWT Forecasting Model	13
REFERENCES	14

Accession For	
NTIS CRA&I	<input checked="" type="checkbox"/>
DTIC TAB	<input type="checkbox"/>
Unannounced	<input type="checkbox"/>
Justification	
By	
Distribution /	
Availability Codes	
Dist	Avail and/or Special
A-1	

## Illustrations

	PAGE
1. Illustration of Operational Domain of Solar Wind Transport Magnetosheath Forecast Model	1

Figures	PAGE
1. Illustration of Sample Simultaneous ISEE 2 and ISEE 3 Data Set for ISEE 2 Orbit 314 Inbound	15
2. Illustration of Sample Simultaneous ISEE 2 and ISEE 3 Data Set for ISEE 2 Orbit 139 Outbound	16
3. Early Validation of Elements of SWT Model: Evaluation of Approximate Newtonian Pressure Formula by Comparison With Gasdynamic Flow Computations	17
4. Early Validation of Elements of SWT Model: Evaluation of Magnetopause Model by Comparison With Other Theoretical Magnetopause Results	18
5. Early Validation of Elements of SWT Model: Evaluation of Gasdynamic Flow Model by Comparison With Laboratory Experiment	19
6. Early Validation of Elements of SWT Model: Evaluation of Gasdynamic Flow Model by Comparison With Observations of Pioneer VI	20
7. Early Validation of Elements of SWT Model: Evaluation of Gasdynamic Flow Model by Comparison With Observations of IMP-1	21
8. Early Validation of Elements of SWT Model: Evaluation of Gasdynamic Flow Model by Comparison With Magnetometer Observations of Bow Shock by Five IMP Spacecraft; 1963-1968	22
9. More Recent Validation of Elements of SWT Model: Evaluation of Convected Magnetic Field Model by Comparison With Pioneer-Venus Observations of Magnetic Field	23
10. More Recent Validation of Elements of SWT Model: Evaluation of Convected Magnetic Field Model at Extreme Low Density Flow Situation ( $n = 0.005/\text{cm}^3$ ) by Comparison With Voyager 2 Observations at Neptune	24
11. Comparison of SWT Model Forecasts and ISEE 2 Observations for Orbit 145 Outbound: ISEE 2 Orbit in Solar Wind Coordinates and Comparison of GSE Velocity Component $V_x$	25
12. Comparison of SWT Model Forecasts and ISEE 2 Observations for Orbit 145 Outbound: GSE Magnetic Field Components	26
13. Illustration of Variation of Solar Wind Sonic, Alfvén and Magnetosonic Mach Number and Magnetopause Nose Radius During ISEE 2 Orbit 145 Magnetosheath Traversal	27
14. Comparison of SWT Model Forecasts and ISEE 2 Observations for Orbit 178 Inbound: ISEE 2 Orbit in Solar Wind Coordinates and Comparison of GSE Velocity Component $V_x$	28

	PAGE
15. Comparison of SWT Model Forecasts and ISEE 2 Observations for Orbit 178 Inbound: GSE Magnetic Field Components	29
16. Comparison of SWT Model Forecasts and ISEE 2 Observations for Orbit 139 Outbound: ISEE 2 Orbit in Solar Wind Coordinates and Comparison of GSE Velocity Component $V_x$	30
17. Comparison of SWT Model Forecasts and ISEE 2 Observations for Orbit 139 Outbound: GSE Magnetic Field Components	31
18. Comparison of SWT Model Forecasts and ISEE 2 Observations for Orbit 319 Outbound: ISEE 2 Orbit in Solar Wind Coordinates and Comparison of GSE Velocity Component $V_x$	32
19. Comparison of SWT Model Forecasts and ISEE 2 Observations for Orbit 319 Outbound: GSE Magnetic Field Components	33
20. Comparison of SWT Model Forecasts and ISEE 2 Observations for Orbit 331 Inbound: ISEE 2 Orbit in Solar Wind Coordinates and Comparison of GSE Velocity Component $V_x$	34
21. Comparison of SWT Model Forecasts and ISEE 2 Observations for Orbit 331 Inbound: GSE Magnetic Field Components	35
22. Comparison of SWT Model Forecasts and ISEE 2 Observations for Orbit 314 Inbound: ISEE 2 Orbit in Solar Wind Coordinates and Comparison of GSE Velocity Component $V_x$	36
23. Comparison of SWT Model Forecasts and ISEE 2 Observations for Orbit 314 Inbound: GSE Magnetic Field Components	37

#### Tables

	PAGE
1. Overview of Combined ISEE 2, ISEE 3 Data Sets for Phase I SWT Model Validation Program: 184 ISEE 2 Magnetosheath Traverses With MP/Bow Shock Crossings; Ordered by Magnetosonic Mach Number	13

## EXECUTIVE SUMMARY

An account is provided of the technical work carried out during the period between delivery of the preliminary Solar Wind Transport Magnetosheath Forecast Model (Phase I SWT model) in November 1991 and the early termination of the contract in July 1993.

The technical work carried out during this period focused on validation of the SWT model and has involved two primary technical tasks: (1) creation of the observational satellite data base against which the model was to be validated, and (2) initial comparative testing of the Phase I SWT model forecasts against these observations. Details of the results obtained from these two technical tasks are discussed.

At the present stage of development, the SWT forecast model remains unqualified for operational use. An outline is provided of the technical tasks required to complete the qualification program.

## 1. OVERVIEW OF SOLAR WIND TRANSPORT MAGNETOSHEATH FORECAST MODEL

### 1.1 Overall Objectives

The overall objectives of the current contract effort is to develop a Solar Wind Transport Magnetosheath Forecast Model (SWT Model) for operational use by the Air Weather Service (AWS) and the Space Forecast Center (SFC). This model will be the first component in a sequential predictive chain that will comprise an integrated space plasma weather forecast system proceeding from  $L_1$  down to low Earth orbit.

The SWT model will proceed from a knowledge of:

- real-time solar wind properties at an upstream spacecraft monitor located approximately at the  $L_1$  libration point
- terrestrial geomagnetic field and certain magnetospheric indices

to forecast the time-dependent plasma and magnetic field properties

- from the upstream monitor to and through the terrestrial bow shock
- throughout the 3-D volume of the magnetosheath region down to and across the magnetopause boundary
- into the outer region of the magnetosphere

The operational domain of the Solar Wind Transport Magnetosheath Forecast model is as shown in the sketch below.

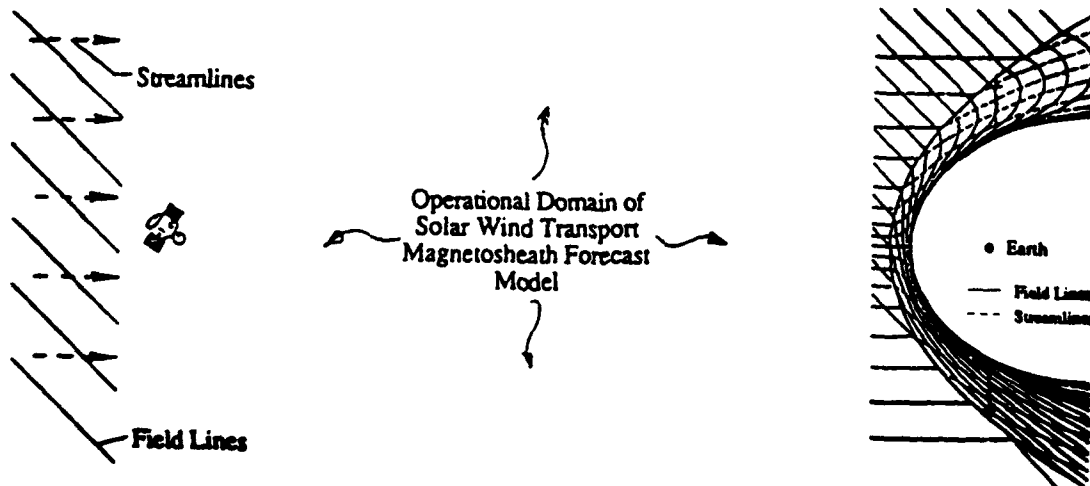


Illustration of Operational Domain of Solar Wind Transport Magnetosheath Forecast Model



The specific output from the SWT model will be:

- location of bow shock and magnetopause surfaces
- plasma and magnetic field properties throughout the magnetosheath region, down to the magnetopause, and into the outer magnetospheric region
- time histories of plasma and magnetic field properties along specific spacecraft trajectories
- input data for Magnetospheric Specification Model and Magnetopause Boundary Layer Model
- selected output displays to facilitate operational use

## 1.2 Operational Elements of SWT Model

The primary challenge in the development of the Solar Wind Transport Magnetosheath Forecast Model is to develop an operational forecasting capability to be approximately 100 times faster than the actual events within the operational domain of the SWT model occur. This will require SWT model operational times of less than a minute, and will provide overall warning times from approximately 10 to 50 minutes depending upon oncoming solar wind conditions.

The objective of the first 18 months of the planned five-year contractual effort was to initially establish all of the essential operational elements of Solar Wind Transport Magnetosheath Forecast Model and to embody them into a preliminary SWT model. These elements are:

### 1. Input Element

- measurement of solar wind properties by upstream monitor located at the  $L_1$  libration point
- determination of input parameters from monitor data for solar wind transport forecast model

### 2. Solar Wind Transport Forecast Element

- determination of plasma and magnetic field properties between upstream monitor and bow shock
- determination of forecast time for Magnetosheath and Bow Shock Forecast Element
- determination of input parameters for Magnetosheath and Bow Shock Forecast Element

### 3. Outer Magnetosphere and Magnetopause Forecast Element

- determination of magnetic field in outer magnetospheric region
- prediction of location of approximate pressure-balanced magnetopause surface
- determination of input parameters for Magnetosheath and Bow Shock Forecast Element

### 4. Magnetosheath and Bow Shock Forecast Element

- prediction of location of bow shock
- prediction of plasma and magnetic field throughout magnetosheath
- determination of input parameters for Forecast Presentation Output Element
- input for MSM Model and other components of forecast system

### 5. Forecast Presentation Output Element

- numerical values
- graphical displays

All of these elements were successfully embodied in a preliminary SWT model that was developed for the purpose of providing utility in the interim period before the final operational SWT model became available. In particular, the preliminary SWT model was specifically constructed to provide all the necessary information regarding model input and output that would be required for real-time operational use with the final operational SWT model. The preliminary SWT model is described in detail in Ref. 1.

Because of the shortness of time from contract start to delivery of the interim SWT model, an essential element that was not possible to be carried out with the preliminary SWT model was the detailed evaluation of SWT model forecasts as well as the actual SWT model validation employing actual satellite data. This task was planned to be the focus of the next technical effort to be carried out on the contract, and was conceived to consist of the following subtasks:

- establishment of a satellite data base that realistically simulates real-time operational data and that would be suitable for SWT model forecast testing
- SWT Model validation by detailed comparison of model forecasts with this observational data base
- identification of elements in the solar wind transport magnetosheath forecast system that require further enhancement
- development and incorporation of all improvements identified as necessary into the final operational SWT model

The work accomplished on these subtasks is described below.

## 2. SATELLITE DATA BASE FOR VALIDATION OF SWT FORECAST MODEL

A study was carried out to identify appropriate candidate archival satellite data sets that would meet the requirements for use in the validation program for the SWT model. These data sets would necessarily be composed of simultaneous observations from at least two spacecraft and provide concurrent observations of both oncoming solar wind plasma and magnetic field conditions and corresponding conditions in the terrestrial magnetosheath.

As a result of this investigation, it was found that the most suitable and available data sets that meet these requirements are the 1978-80 ISEE 2 and 3 observations. A large library of archival results from these ISEE spacecraft is currently available. However, the actual assembly of the satellite data base sufficient for validation of the SWT model, which would necessarily involve the correlation of a large number (of the order of ~200) of simultaneous ISEE 2 and ISEE 3 data sets from this library, represents a substantial effort. This is so since the individual ISEE spacecraft data sets have to be searched separately to ascertain data continuity, completeness and appropriateness, and then these same ISEE data sets need to be correlated to insure simultaneous coverage of both solar wind and magnetosheath. Furthermore, such an effort is peripheral to the SWT model developments and improvements needed in the validation effort. Consequently, in order to ameliorate the impact on contract resources, we have established a joint collaborative program with UCLA and Prof. C. T. Russell and Dr. G. Le of the Geophysics Dept. Under this program, RMA and UCLA will jointly identify the simultaneous ISEE data sets, UCLA will provide the actual numerical ISEE data sets to RMA, and RMA will share the comparative results with UCLA. The result of this collaborative program is that RMA will acquire a sufficiently extensive satellite data base to validate the SWT model at a minimum expense to the project.

We have now carried out the identification of 184 simultaneous ISEE solar wind and magnetosheath data sets that are both appropriate and

sufficient for the SWT model validation program. These data sets involve ISEE 2 observations of the magnetosheath with simultaneous ISEE 3 observations of the oncoming solar wind. Each of the ISEE 2 data sets involves at least one magnetopause crossing and may contain in addition one or more bow shock crossings. The time intervals spanned by the ISEE 2 magnetosheath traversals vary from about 4 to 42 hours and the traversals are located in the dayside magnetosheath. For these observations, ISEE 3 is nominally located in the solar wind near the L<sub>1</sub> libration point. All the observational data for both ISEE 3 and ISEE 2 for both plasma and magnetic field are available at 1 min. intervals.

Table 1 provides an overview of the combined ISEE 3 and ISEE 2 data sets. A summary is provided of conditions both in the solar wind and at the Earth (Dst, dipole tilt) at the time of the initial ISEE 2 magnetopause crossing. The data sets are ordered by increasing magnetosonic Mach number and span the range from  $2.1 \leq M_{ms} \leq 8.2$ .

Figures 1 and 2 below provide illustrations of sample simultaneous data sets from this data base. Figure 2 displays data set #003 which corresponds to ISEE 2 Orbit 314 inbound. Magnetosheath data from ISEE 2 are shown by the thin lines, while corresponding solar wind data from ISEE 3 is superimposed and shown as thick lines. The ISEE 3 data for this illustration has been uniformly time shifted forward by 50 minutes to allow for the arrival time lag. The data illustrated in Figure 1 are for moderately unsteady solar wind plasma conditions as evidenced by the observed density variations, but for fairly steady IMF. These data are for relatively low solar wind magnetosonic Mach number conditions, i.e.  $M_{ms} \sim 2$ . Figure 2 displays corresponding ISEE 3 and ISEE 2 data for more typical solar wind magnetosonic Mach number conditions, i.e.  $M_{ms} \sim 6$ , with conditions in the solar wind fairly steady for both the plasma and IMF.

The current status of this ISEE 2 and ISEE 3 data base is that the data base is currently archived in total at UCLA. Selected sets of the data base which are described below have been transferred to RMA for initial comparative testing of the SWT forecast model. Final transfer of the complete archival data base to RMA has not been carried out.

### 3. SWT MODEL VALIDATION PROGRAM

#### 3.1 Previous Validation of Elements of the SWT model

The primary purpose of the SWT model validation program is to assess and qualify the accuracy of the SWT model forecasts in situations that simulate as closely as possible the real-time operational environment that the model will be used in. Previous studies have served to successfully verify a number of elements embodied in the current SWT model. For example, validation of the methodology employed in the development of the approximate pressure-balanced magnetopause shape, as shown in Figure 3, which underlies the entire basis of the gasdynamic convected field model employed in the SWT model to determine the magnetosheath plasma and magnetic field, was made early on in Ref. 2. Similarly, validation of the accuracy of the Briggs-Spreiter magnetopause model incorporated in the SWT model was successfully made in Ref. 3 by comparison with other theoretical magnetopause model results. These results are summarized in Figure 4. An important early evaluation of the gasdynamic plasma flow model employed in the SWT model

was reported in Ref. 4 where a comparison of model-predicted with laboratory-observed bow shock shape about a model magnetopause was made. These results are shown in Figure 5. One of the initial evaluations of detailed plasma properties in the magnetosheath as predicted by the gasdynamic model was made by comparison with observations of Pioneer VI plasma data (Ref. 4) as shown in Figure 6, and also with IMP-1 data (Ref. 4) and is shown in Figure 7. Another initial validation of the gasdynamic flow model but this time using magnetometer rather than plasma observations of the bow shock by five IMP spacecraft from 1963-68 was made in Ref. 5 and is shown in Figure 8. A more recent validation of the convected magnetic field model employed in the SWT model was reported in Ref. 6 and is illustrated in Figure 9 where a comparison of the predicted magnetic field along the Pioneer-Venus spacecraft trajectory in the Venusian magnetosheath was made with PVO magnetometer observations. Another successful recent validation of the convected magnetic field model is reported in Ref. 7 and illustrated in Figure 10, where comparison of the predicted magnetic field along the Voyager 2 spacecraft trajectory was made with Voyager 2 magnetometer observations. A recent summary of comparisons of various elements embodied in the SWT model with observations from a variety of spacecraft and solar wind/planetary interactions throughout the solar system are provided in Refs. 7 and 8. All of these previous comparisons have served to provide a firm basis for the preliminary successful validation of the accuracy of a number of elements of the SWT model.

### 3.2 Current Validation Results of the SWT Model

The one important aspect that was not possible to investigate in these previous studies due to the absence of an appropriate satellite data base was the use of continuous oncoming solar wind plasma and magnetic field information as input to the SWT model. Prior to the current study, this was the one crucial feature of the operational forecasting problem that had never been previously tested against the various elements embodied in the present SWT model. The key advantage of the SWT model as employed in an operational mode, however, lies in this very aspect. That is, the ability of the currently-configured SWT model to employ short time-interval (of the order of 1 min.) solar wind input data to rapidly predict (in a few CPU secs.) the global magnetosheath plasma and field properties, including in particular the location of the magnetopause and bow shock surfaces and conditions at specific spacecraft orbital locations within the global magnetosheath, makes the model uniquely valuable for real-time operational use.

The general plan for the SWT model validation program is to employ the simultaneous ISEE 3 solar wind data as input to the SWT model and then to make comparisons of the plasma and magnetic field properties forecast by the model at the ISEE 2 spacecraft orbital locations in the magnetosheath with the ISEE 2 observations of plasma and magnetic field. In order to qualify the SWT model for operational use, it will be necessary to employ approximately half of the 184 simultaneous ISEE 3 and ISEE 2 data sets contained in the data base. It was planned that the initial comparative testing would be made for selected data sets corresponding to solar wind conditions believed favorable for good SWT model forecasting. Subsequent comparisons would then be made for selected data sets corresponding to solar wind conditions believed to be increasing less favorable for good forecasting, i.e. low Mach number, large IMF, very unsteady plasma and magnetic field, etc.

To date, we have now carried out detailed comparisons of the SWT model forecasts with the ISEE observations for 6 of these simultaneous data sets. These validation studies demonstrate that the Phase I SWT model forecasting results are generally in good agreement with the ISEE 2 magnetosheath observations. They have also, however, disclosed a number of deficiencies.

In particular, the global magnetic field forecast of the Phase I SWT model in the vicinity of the magnetopause, particularly at low solar wind Alfvén Mach numbers, was found to display a consistent systematic discrepancy with the ISEE observations. The source of a major part of this discrepancy has been identified as due to a previously-known spurious magnetic singularity at the magnetopause that is contained in the basic gasdynamic convected magnetic field model. A provisional procedure has been preliminarily developed to diminish the effects of this singularity. This procedure is based on the known physical constraint that the magnetosheath magnetic field at the magnetopause cannot exceed the local confined magnetospheric magnetic field on the interior surface of the magnetopause at that location. This procedure has been initially tested against the ISEE 2 data, and the forecasts of the magnetic field provided by this modification, as shown in Figures 12 to 23 below, provide a significant improvement over those provided by the Phase I SWT model.

In addition, initial comparisons indicate that superior SWT model forecasts are achieved at low solar wind Alfvén Mach numbers by employing the magnetosonic rather than sonic Mach number as input to the SWT model. Additionally, it has been found that employing the magnetosonic Mach number does not alter the agreement of the SWT model forecasts for situations at high solar wind Alfvén Mach numbers. In all of the comparisons shown below in Figures 11-23, the magnetosonic Mach number has been employed as input to the gasdynamic calculation in the SWT model.

In Figures 11 and 12, we provide results of the first comparisons of the SWT model forecasts and ISEE 2 observations for ISEE 2 orbit 145 outbound. This data set (#178) was selected as one of the initial candidates for the validation study as it corresponded to solar wind conditions that were believed favorable for good SWT model forecasts; that is, high magnetosonic Mach number ( $M_{ms} \sim 7.1$ ),  $B_z$  northward, steady solar wind plasma conditions, fairly steady IMF, and single bow shock and magnetopause crossings by ISEE 2. The plot on the left of Figure 11 provides a view of the ISEE 2 spacecraft orbit as seen in the solar wind (X,R) coordinate system fixed to the magnetopause that is employed in the global magnetosheath computations. Such a view of the spacecraft trajectory is quite informative as it immediately exhibits the magnitude of the effects caused by unsteadiness in the solar wind dynamic pressure and solar wind direction. These are revealed, respectively, in this view of the spacecraft trajectory by: (1) abrupt radial jumps in the spacecraft trajectory corresponding to the sudden inflation or deflation of the magnetopause obstacle size in response to solar wind dynamic pressure changes, and (2) abrupt lateral excursions of the spacecraft trajectory corresponding to sudden changes in the solar wind direction. As is evident in the plot in Figure 11, for the time that the ISEE 2 spacecraft spent in the magnetosheath during this orbit, the direction of the solar wind underwent several abrupt changes. The comparison of the prediction from the SWT model for the velocity component  $V_x$  in GSE

coordinates with the ISEE 2 fast plasma analyzer displays very good agreement for the location of both the bow shock and magnetopause surfaces, and very good agreement for the magnitude of the velocity component for most of the magnetosheath crossing. Some disagreement does appear between SWT predictions and observations in the vicinity of the magnetopause surface. We have no explanation for this. As will be seen from the comparisons for the other five case studies, the discrepancies of SWT model forecasts with the ISEE 2 fast plasma analyzer observations for velocity exhibit no systematic trends. In some cases, the agreement is essentially perfect, while for others some discrepancies may appear. These discrepancies might in fact be attributable primarily to the instrument since we have discovered what appears to be a systematic error in the magnitude (underreported by almost a factor 2) of the plasma density reported by the ISEE 2 fast plasma analyzer for all of the case studies that have been undertaken. Figure 12 provides corresponding comparison of the SWT model forecast and the ISEE 2 magnetometer for the magnetic field components in GSE coordinates. As with the plasma velocity comparison, the magnetic field comparisons are very good for most of the magnetosheath region, with some disagreement in the vicinity of the magnetopause. These comparisons confirm the good agreement of the locations of both the bow shock and magnetopause surfaces already observed in the plasma velocity comparisons in Figure 11. To provide some indication of the steadiness of the solar wind parameters during the ISEE 2 magnetosheath crossing for this orbit, we have prepared Figure 13 which provides the variation of the solar wind sonic, Alfvén and magnetosonic Mach numbers during the ISEE 2 magnetosheath traversal. Also shown in Figure 13 is the pressure-balanced magnetopause nose radius  $R_0$ , which provides an indication of the inflation and deflation undergone by the magnetopause during this time interval. As can be observed from Figure 13, while the solar wind conditions are reasonably steady during this time interval, they are by no means absolutely quiescent.

Figures 14 and 15 provide corresponding comparisons of SWT model forecasts and ISEE 2 observations for orbit 178 inbound. This data set (#181) was selected as one of the candidates for the initial validation study since although this orbit contains solar wind conditions that were considered mostly favorable for good SWT model forecasts, it also contains some solar wind conditions believed unfavorable that would subsequently serve as a further test of the SWT model. For this case, the solar wind conditions are: high magnetosonic Mach number ( $M_{ms} \sim 8.0$ ),  $B_z$  northward, moderately unsteady solar wind plasma conditions, moderately unsteady IMF, and multiple bow shock crossings were observed by ISEE 2. In Figure 14, we observe from the plot of the ISEE 2 orbit in solar wind coordinates that due to inflation of the magnetopause the spacecraft essentially loiters about the bow shock resulting in the multiple bow shock crossings observed in the plasma velocity comparisons shown in the plot on the right. The ISEE 3 data gap during the period when the spacecraft initially crosses the bow shock undoubtedly causes the discrepancy for the first predicted bow shock crossing. However, the prediction of the later multiple bow crossings by the SWT model and the magnitude of the velocity component throughout the magnetosheath is in excellent agreement with the ISEE 2 fast plasma analyzer observations. Figure 15 also confirms this high level of agreement for the magnetic field components as well, and in addition shows that even a difficult detail, such as the multiple bow shock crossing at about 14.0 hours UT, is remarkably captured by the SWT model magnetic field forecasts. Both the level and variation of the all of the magnetic

field components are exceptionally well predicted for this case in which there exists moderate unsteadiness in both the oncoming solar wind plasma flow as well as the IMF.

Figures 16 and 17 display the analogous comparisons for ISEE 2 orbit 139 outbound. This data set (#145) was selected as one of the candidates for this initial validation study as it corresponded to solar wind conditions that were also believed favorable for good SWT model forecasts: that is, high magnetosonic Mach number ( $M_{ms} \sim 5.6$ ),  $B_z$  northward, steady solar wind plasma conditions, fairly steady IMF, and single bow shock and magnetopause crossings by ISEE 2. In Figure 16, we note from the plot of the ISEE 2 trajectory in solar wind coordinates that a high number of directional changes in the oncoming solar wind occur during the ISEE 2 magnetosheath traverse of this orbit. Nevertheless, the comparison of the SWT model forecast and ISEE 2 observed axial velocity component exhibits very good agreement for location of both bow shock magnetopause crossings. In addition, the trend of the variation of this velocity component is well predicted, although the magnitude appears to be off by a constant factor throughout the magnetosheath. As before, we have no explanation for this discrepancy. In Figure 17, however, the three components of predicted magnetic field display excellent agreement with the ISEE 2 observations across the entire magnetosheath. This is a key reason why we suspect errors in the ISEE 2 fast plasma analyzer data. Recall that in the SWT model, the convected magnetic field is the last global quantity to be calculated. This is so since the convected field model incorporated in the SWT forecast model requires knowledge of both the velocity and density fields throughout the magnetosheath before the computation of the magnetic field can be initiated. Consequently, any error in the flow field computation or any inadequacy in either the flow field or magnetic field computation would be displayed most prominently in the magnetic field comparisons. However, for this case, as well as others studied here in which a discrepancy appears in the comparisons between the SWT model predictions and ISEE 2 observations for the magnetosheath velocity, this discrepancy in velocity is not carried over into the magnetic field comparisons which almost uniformly display excellent agreement. We note, furthermore, that the agreement between SWT model forecast and observation is also quite good in all cases studied for the locations of both the bow shock and magnetopause surfaces. It is not possible for the SWT model forecasts to be accurate in predicting the locations of the bounding surfaces of the magnetosheath as well as to be accurate in the predictions of the vector magnetic field throughout the magnetosheath while simultaneously containing a significant error in the magnetosheath vector velocity. Consequently, we believe that there exist errors in the ISEE 2 plasma analyzer data for the vector velocity as well as for the density. Further study of this aspect of the ISEE 2 observations is clearly needed.

In Figures 18 thru 23, analogous comparisons are made between the SWT model forecasts and ISEE 2 magnetosheath observations for three additional case studies all of which involve low solar wind magnetosonic Mach number, i.e.  $2.2 \leq M_{ms} \leq 3.0$ . These data sets (#009, #007, #003) were purposely selected as candidates for this initial validation study in order to provide a further challenge to the SWT model since the assumptions under which the basic gasdynamic convected magnetic field computational model used to determine the global magnetosheath plasma and magnetic field properties in the SWT model is based become highly strained at low magnetosonic Mach number. However, with the use of the



solar wind magnetosonic rather than sonic Mach number in the global gasdynamic plasma calculation, the predicted results for both plasma and magnetic field properties in the magnetosheath for all 3 of these case studies are in very good agreement with the ISEE 2 observations. This result was not anticipated, and warrants further study to evaluate the reasons underlying this agreement. Figures 18 and 19, which correspond to ISEE 2 orbit 319 outbound, display results for the longest ISEE 2 magnetosheath traversal interval studied in all of the case studies undertaken, i.e. 41 hours. Figure 18 shows very good agreement between the SWT model forecast and ISEE 2 observation for the velocity component, and Figure 19 confirms that agreement for the vector magnetic field. Note in particular the extreme variation in the  $B_z$  component displayed in the ISEE 2 data in Figure 19 and which is accurately captured by the SWT model forecasts. Figures 20 and 21 display analogous comparisons for ISEE 2 orbit 331 inbound. Figure 20 shows a remarkable agreement between the SWT model forecasts and ISEE 2 observations for the axial velocity component, with the only exception being the SWT model forecast of a bow shock crossing at about 7:30 UT which does not appear in the observations. Figure 21 which displays the comparison of the vector magnetic field components exhibits the same excellent agreement between model forecasts and observations. Figures 22 and 23 display the final comparisons, and correspond to solar wind conditions for the lowest magnetosonic Mach numbers of all the case studies undertaken. Again, the agreement between the SWT model forecasts and the ISEE 2 observations for the axial velocity component shown in Figure 22 is very good, as is that for the vector magnetic field illustrated in Figure 23. The only feature of these three case studies that displays any systematic discrepancy between model forecast and observation at all is that the magnitude of the predicted magnetosheath magnetic field at low magnetosonic Mach numbers is somewhat underpredicted compared to the observations. A correction parameterized by magnetosonic Mach number and based on an extended series of case studies should be developed in order to improve this.

#### 4. CONCLUSIONS AND RECOMMENDATIONS

##### 4.1 Status of SWT Validation Program

The observational data base required for the validation of the SWT forecasting model has now been established. The data base is comprised of a total of 184 ISEE 2 and simultaneous ISEE 3 data sets that involve solar wind plasma and field measurements from the ISEE 3 spacecraft and corresponding plasma and field magnetosheath measurements from the ISEE 2 spacecraft. Case studies to investigate the accuracy of the SWT model forecasts have been initiated by using selected sets from this data base. Comparative results have currently been obtained for 6 of these ISEE 2 and ISEE 3 data sets. These selected sets have involved solar wind conditions anticipated to be both favorable and unfavorable for good SWT forecasts. The preliminary results from these case studies have in general been very favorable. Even from this small number of cases studied so far, however, several important features in both the plasma and magnetic field procedures employed in the interim Phase I SWT model have been identified that require improvement. Provisional procedures have been developed as far as possible during this period to improve these methods, but require both further development and study.

#### 4.2 Final Qualification of SWT Forecasting Model

At the present development stage, the SWT forecasting model remains unqualified for operational use. The study to establish figures of merit for the model that would provide estimates of the quality of the real-time SWT forecasts in an operational environment has not been initiated.

The primary technical tasks remaining to complete the SWT model validation program and qualify the model for operational use consists of the following:

- completion of the SWT model comparative forecasts for a minimum of half of the currently established ISEE 2 and ISEE 3 observational data base
- development and incorporation of all improvements identified as necessary from the above comparative study for the plasma and magnetic field computational models embodied in the Phase I SWT model
- establishment of figures of merit for the SWT model forecasts as a function of solar wind parameters

## REFERENCES

1. Stahara, S. S., R. R. Rachiele, G. A. Molvik, and J. R. Spreiter: Development of a preliminary solar wind transport magnetosheath model-Interim report, RMA TR109, Nov. 1991.
2. Spreiter, John R., Summers, Audrey L. and Alksne, Alberta Y., Hydrodynamic flow around the magnetosphere. *Plan. and Space Sci.*, 14, 223-253, 1966.
3. Spreiter, J. R., and B. R. Briggs, Theoretical determination of the form of the boundary of the corpuscular stream produced by interaction with the magnetic dipole of the earth, *J. Geophys. Res.*, 67, 37-51, 1962.
4. Spreiter, J. R., A. Y. Alksne, and A. L. Summers, External aerodynamics of the magnetosphere, in *Physics of the Magnetosphere*, edited by R. L. Carovillano, J. F. McClay, and H. R. Radoski, pp. 304-378, D. Reidel, Hingham, Mass., 1968.
5. Fairfield, D. H., Average and unusual locations of the earth's magnetopause and bow shock, *J. Geophys. Res.*, 76, 6700-6712, 1971.
6. Luhmann, J. G., R. J. Warniers, C. T. Russell, J. R. Spreiter, and S. S. Stahara: A Gas Dynamic Magnetosheath Field Model for Unsteady Interplanetary Fields: Application to the Solar Wind Interaction with Venus, *J. Geophys. Res.*, 91, 3001-3010, 1986.
7. Spreiter, J. R., and S. S. Stahara, Gasdynamic and magnetohydrodynamic modeling of the magnetosheath: A tutorial, COSPAR Proceedings, Sept. 1992.
8. Spreiter, J. R., and S. S. Stahara, Computer modeling of solar wind interaction with Venus and Mars, in *Comparative Study of Venus and Mars: Atmospheres, Ionospheres and Solar Wind Interactions*, edited by J. G. Luhmann and M. Tatrallyay, AGU Monograph 66, 1992.

Event #	Year	Day	Time (ISEE 2)	Orbit #	Crossings	M GSM	V GSM	Z GSM	Bz	Tdopm (ISEE3)	Tdopm (ISEE3)
1	181	78	272	13:00:00.000	144	1	6.67283	-1.58628	5.16811	1	11.800
2	244	79	335	12:27:00.000	323	1	1.62418	-9.57197	7.27744	2	10.900
3	238	79	315	20:42:00.000	314	1	11.29260	-2.38713	-1.59949	3	11.300
4	99	78	269	17:30:00.000	142	1	10.43800	6.34953	-0.6612	2	6.400
5	213	79	280	11:10:00.000	300	1	8.31463	-2.00328	5.83506	3	12.900
6	115	78	303	16:12:00.000	157	1	5.27740	-6.02612	6.54204	1	3.500
7	257	79	356	12:15:00.000	331	3	6.97326	-8.66535	-4.0585	2	11.000
8	920	78	291	15:45:00.000	152	1	4.50786	-3.96191	5.38725	2	20.300
9	239	79	327	18:15:00.000	319	1	11.65110	-5.91679	-1.04007	1	1.600
10	212	78	288	02:22:00.000	299	1	7.23547	3.74639	-3.05407	1	5.900

n (s. wind) (ISEE3)	v (s. wind) (ISEE3)	p u^2 (s. wind) (ISEE3)	Time (ISEE3)	a (s. wind) (ISEE3)	v (s. wind) (ISEE3)
1	1.400	791.900	1.550E-8 272 12:29:59		
2	2.498	363.400	5.491E-9 335 11:38:00		
3	6.818	423.300	2.030E-8 315 19:54:59		
4	2.878	510.100	8.995E-9 269 16:58:00		
5	6.748	419.500	1.981E-8 280 10:25:00		
6	4.330	376.600	1.826E-8 303 15:20:00		
7	11.120	345.700	2.219E-8 356 11:10:00		
8	4.780	428.100	1.463E-8 291 14:55:00		
9	4.060	316.300	6.783E-9 327 17:15:00		
10	18.520	383.000	2.577E-8 288 01:25:00		394.000

p u^2 (s. wind) (IMPB)	Time (IMPB)	Dist	Dipole tilt (deg)	BT (ISEE3)	Mms (ISEE3)
1		-211	4.900	20.610	2.120
2		-3	-15.300	11.440	2.180
3		14	-12.200	22.850	2.207
4		-70	10.100	13.560	2.402
5		-26	-2.400	17.720	2.656
6		-111	-2.000	12.330	2.698
7		14	-10.000	16.150	2.929
8		-59	2.000	13.480	2.963
9		1	-9.800	8.540	2.974
10	3.215E-8 288 02:12:30	-40	-15.300	16.930	3.053

$$B_z = \begin{bmatrix} 1 \\ 2 \\ 3 \end{bmatrix} = \begin{bmatrix} \text{Southward} \\ \text{Equatorial} \\ \text{Northward} \end{bmatrix}$$

Table 1. Overview of Combined ISEE 2, ISEE 3 Data Sets for Phase I  
SWT Model Validation Program: 184 ISEE 2 Magnetosheath  
Traverses With MP/Bow Shock Crossings: Ordered by  
Magnetosonic Mach Number

Lineal	Year	Day	Time (ISTE3)	Orbit	Wavelength	B (ISTE3)	V (ISTE3)	Z (ISTE3)	Wavelength (ISTE3)	Y (ISTE3)
177	185	78	201 18:34:00.000	147	3	8.56551	4.00050	-7.5010	3	4.700
178	182	78	275 00:10:00.000	145	1	9.00013	-3.30266	5.23075	3	12.900
179	129	78	331 21:43:00.000	166	5	10.15510	-5.52310	3.7499	1	14.000
180	123	78	319 22:55:00.000	163	3	11.06170	-5.22225	7.7642	3	10.500
181	148	78	355 10:32:00.000	170	1	7.21478	-9.06017	-3.9390	2	12.900
182	145	78	365 07:20:00.000	182	3	5.49740	-17.53150	1.52060	3	26.000
183	266	80	5 19:47:00.000	337	15	4.62145	-9.71909	-4.65471	2	24.200
184	922	79	189 00:27:00.000	261	1	-3.96170	14.72000	7.6413	3	3.400

a (s. wind)	(ISTE3)	w (s. wind)	(ISTE3)	p w^2 (s. wind)	(ISTE3)	Time (ISTE3)	n (s. wind)	(ISTE3)	m (s. wind)	(ISTE3)
177	21.600		365.000		4.004E-3	201 17:35:00				
178	4.370		499.100		1.010E-3	274 23:24:59				
179	2.590		544.000		1.204E-3	331 21:04:59		3.590		552.000
180	3.090		409.000		1.559E-3	319 22:14:59				
181	3.340		573.400		1.470E-3	355 17:50:00				
182	3.550		601.100		2.150E-3	365 06:49:59				
183	2.650		509.100		1.536E-3	005 19:05:00		3.370		584.000
184	12.100		402.300		4.735E-3	100 23:35:00				

p w^2 (s. wind)	(ISTE3)	Time (ISTE3)	Orbit	Wavelength (deg)	BT (ISTE3)	Time (ISTE3)
177			-11	4.000	1.270	6.910
178			-43	-8.500	4.530	7.064
179	1.027E-3	331 21:37:30	-50	-10.700	3.760	7.445
180			-30	-19.900	3.040	7.657
181			-30	-13.000	3.120	7.970
182			-47	-31.900	5.700	8.093
183	1.919E-3	005 19:09:30	-2	-14.200	3.940	8.012
184			2	17.000	4.300	8.147

$\theta_2 = \begin{bmatrix} 1 \\ 2 \\ 3 \end{bmatrix} = \begin{bmatrix} \text{Southward} \\ \text{Equatorial} \\ \text{Northward} \end{bmatrix}$

Table 1. Concluded.

# **Data Set #003: ISEE 3 Solar Wind + ISEE 2 Magnetosheath Data**

ISEE 2 (Thin line) and ISEE 3 (Thick line), Delta Time = 50 min

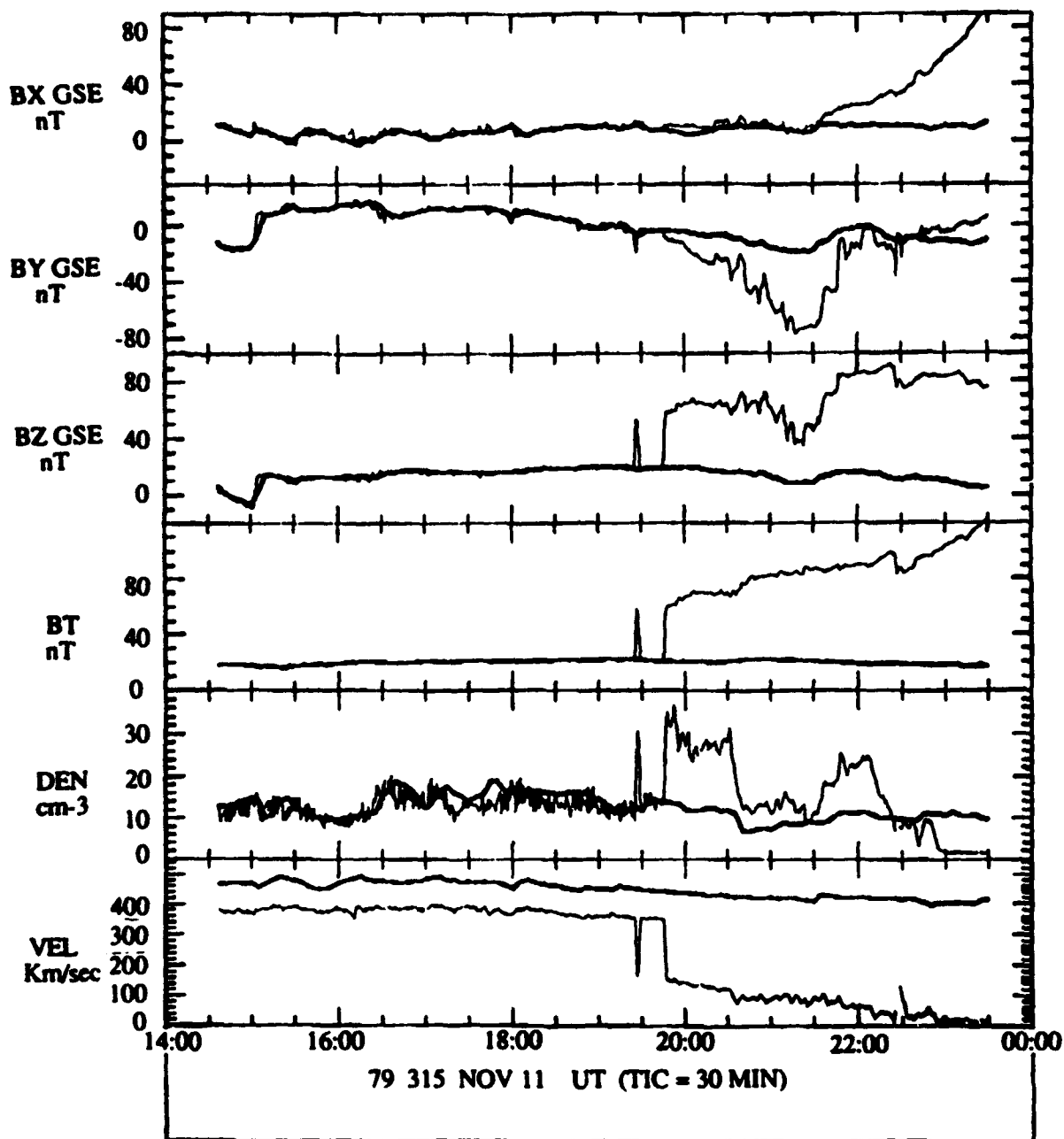


**Figure 1.** Illustration of Sample Simultaneous ISEE2 and ISEE 3 Data Set For ISEE 2 Orbit 314 Inbound

# **Data Set #145: ISEE 3 Solar Wind + ISEE 2 Magnetosheath Data**

ISEE 2 (Thin line) and ISEE 3 (Thick line), Delta Time = 50 min

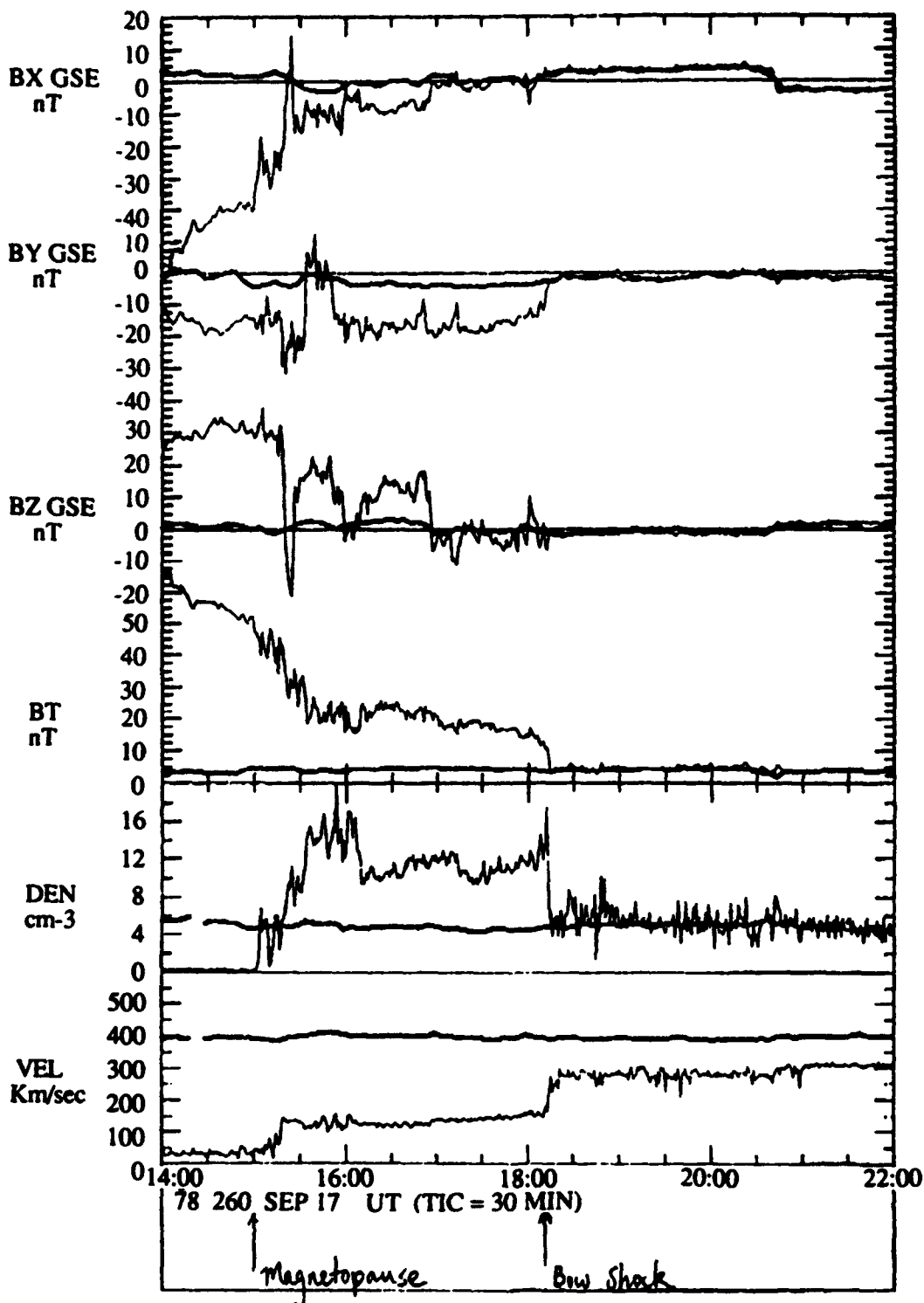
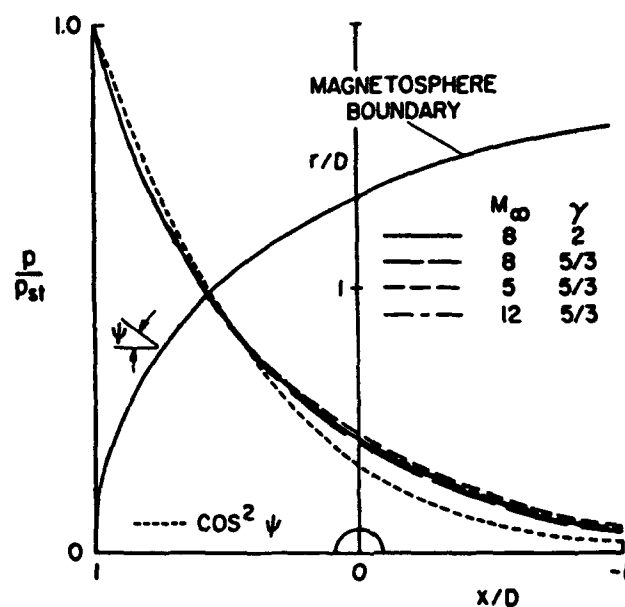


**Figure 2.** Illustration of Sample Simultaneous ISEE2 and ISEE 3 Data Set For ISEE 2 Orbit 139 Outbound



Comparison of exact and approximate pressure distributions on magnetosphere boundary

Figure 3. Early Validation of Elements of SWT Model: Evaluation of Approximate Newtonian Pressure Formula by Comparison With Gasdynamic Flow Computations



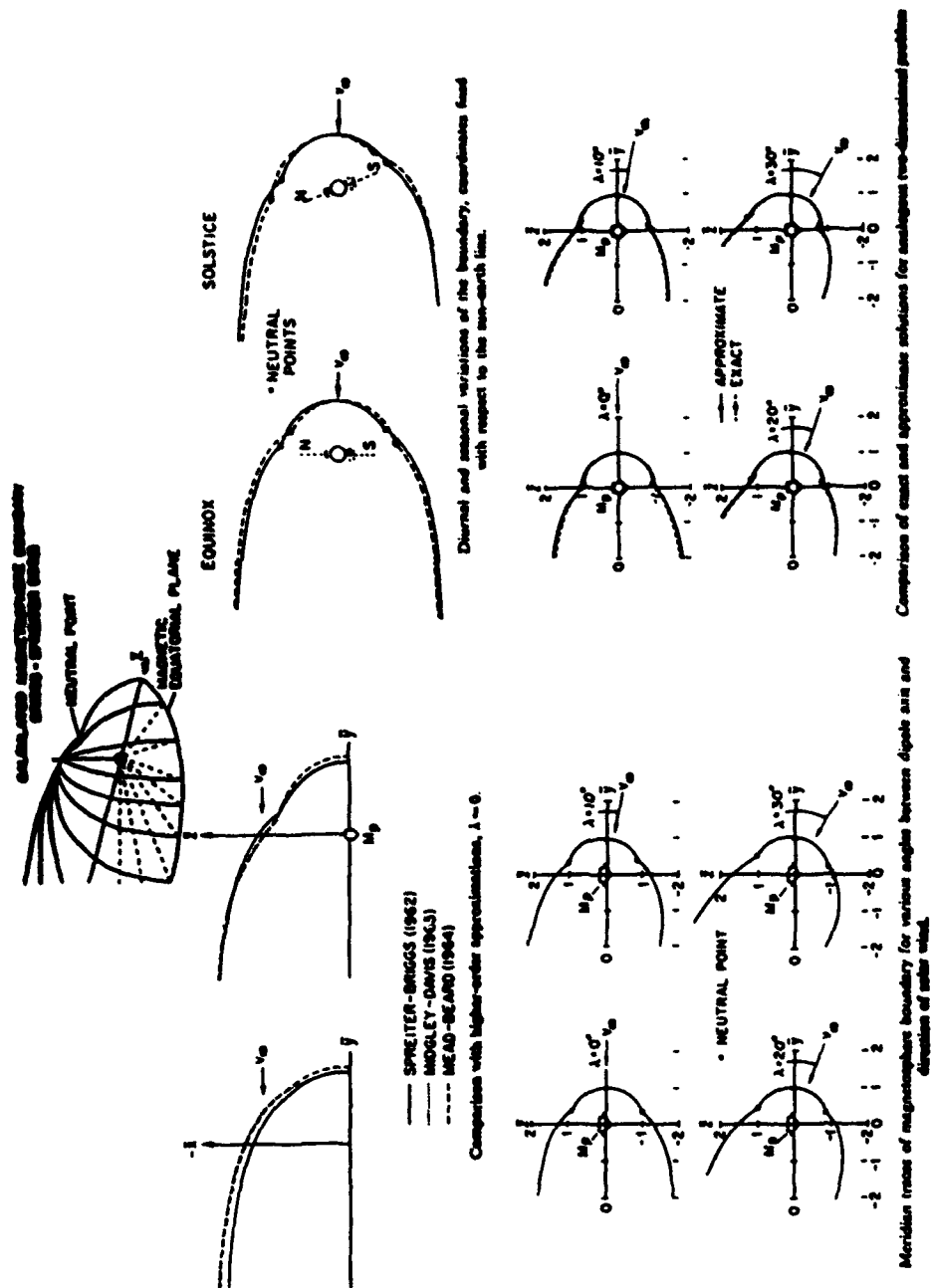
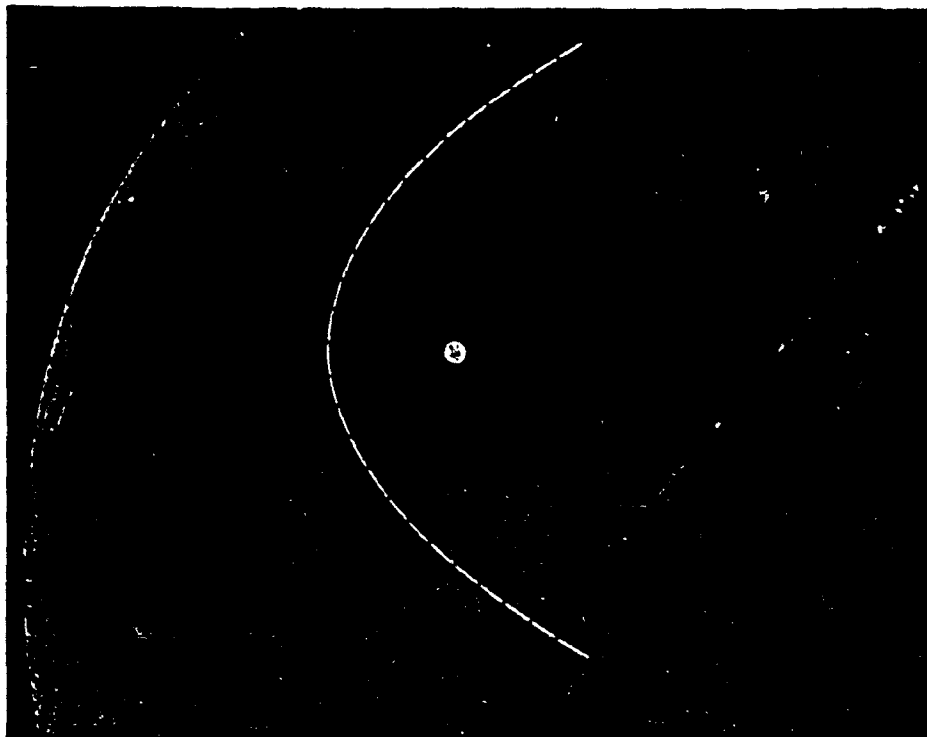


Figure 4. Early Validation of Elements of SMT Model: Evaluation of Magnetopause Model by Comparison With Other Theoretical Magnetopause Results



Comparison of calculated and observed positions of bow wave of model magnetosphere in flight at Mach number 4.65 through argon ( $\gamma = 5/3$ ). Equatorial plane (SPARTAN and HYATT, 1963),  $p_0/p_\infty = .1$ .

**Figure 5.** Early Validation of Elements of SHT Model: Evaluation of Gasdynamic Flow Model by Comparison With Laboratory Experiment

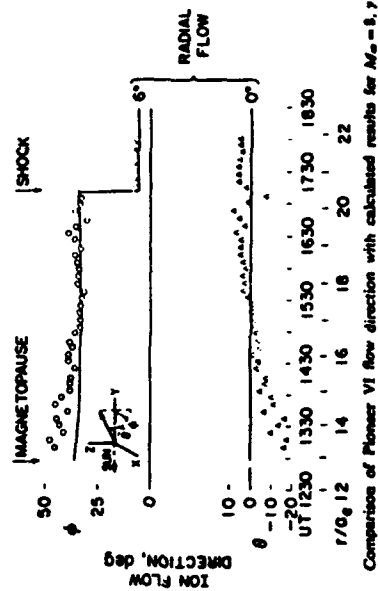
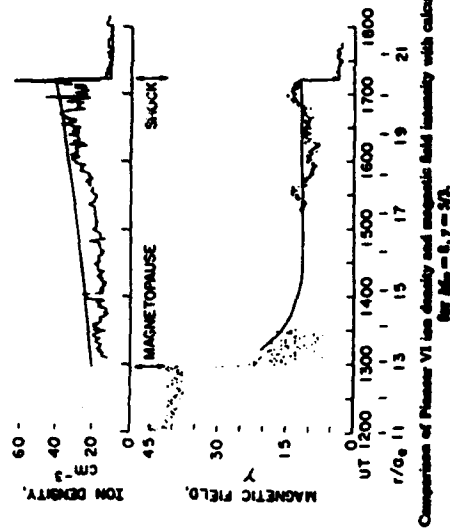
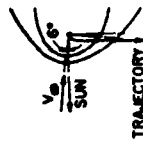
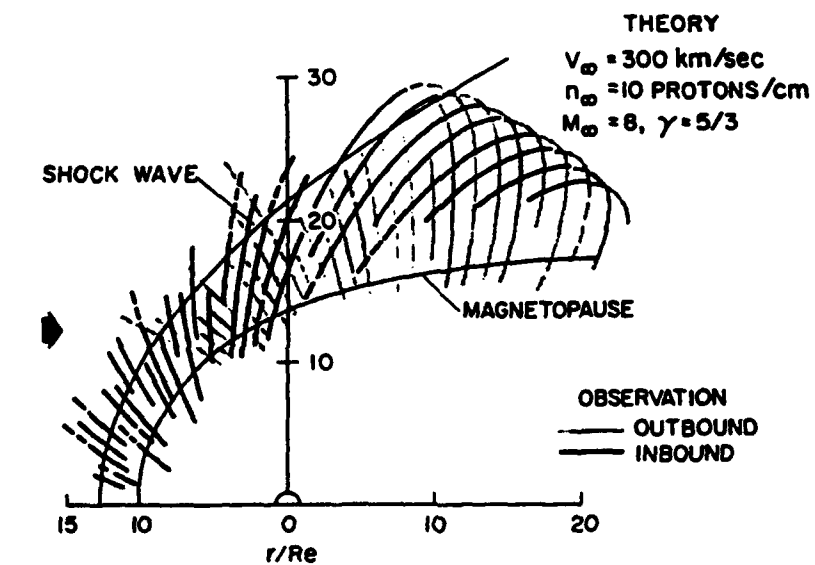
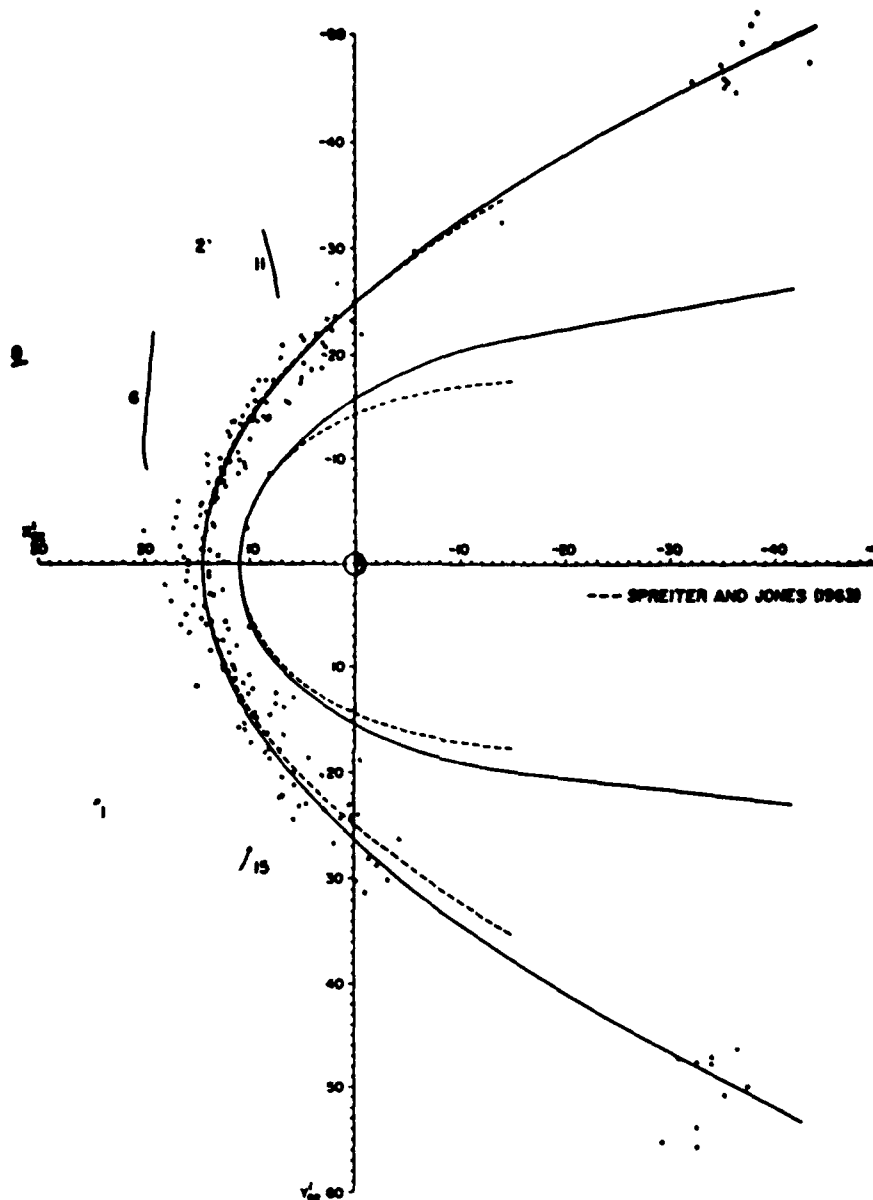


Figure 6. Early Validation of Elements of SNT Model: Evaluation of Gasdynamic Flow Model by Comparison With Observations of Pioneer VI



IMP-I plasma probe measurements of shock wave and magnetosphere boundary crossings

Figure 7. Early Validation of Elements of SWT Model: Evaluation of Gasdynamic Flow Model by Comparison With Observations of IMP-1



Position of the bow shock in the solar ecliptic plane as determined by measurements on five Imp spacecraft, 1963-1968. Crosses represent the average location on individual passes, and the solid line hyperbola represents the best-fit curve to the points.  $|Z_{\text{sc}}| < 7 R_E$ . Points have been rotated by  $4^\circ$  to remove the effects of aberration due to the earth's motion about the sun. The line segments beyond the average shock position represent the positions of unusually distant bow-shock locations.

**Figure 8. Early Validation of Elements of SMT Model: Evaluation of Gasdynamic Flow Model by Comparison With Magnetometer Observations of Bow Shock by Five IMP Spacecraft: 1963-1968**

# Steady IMF

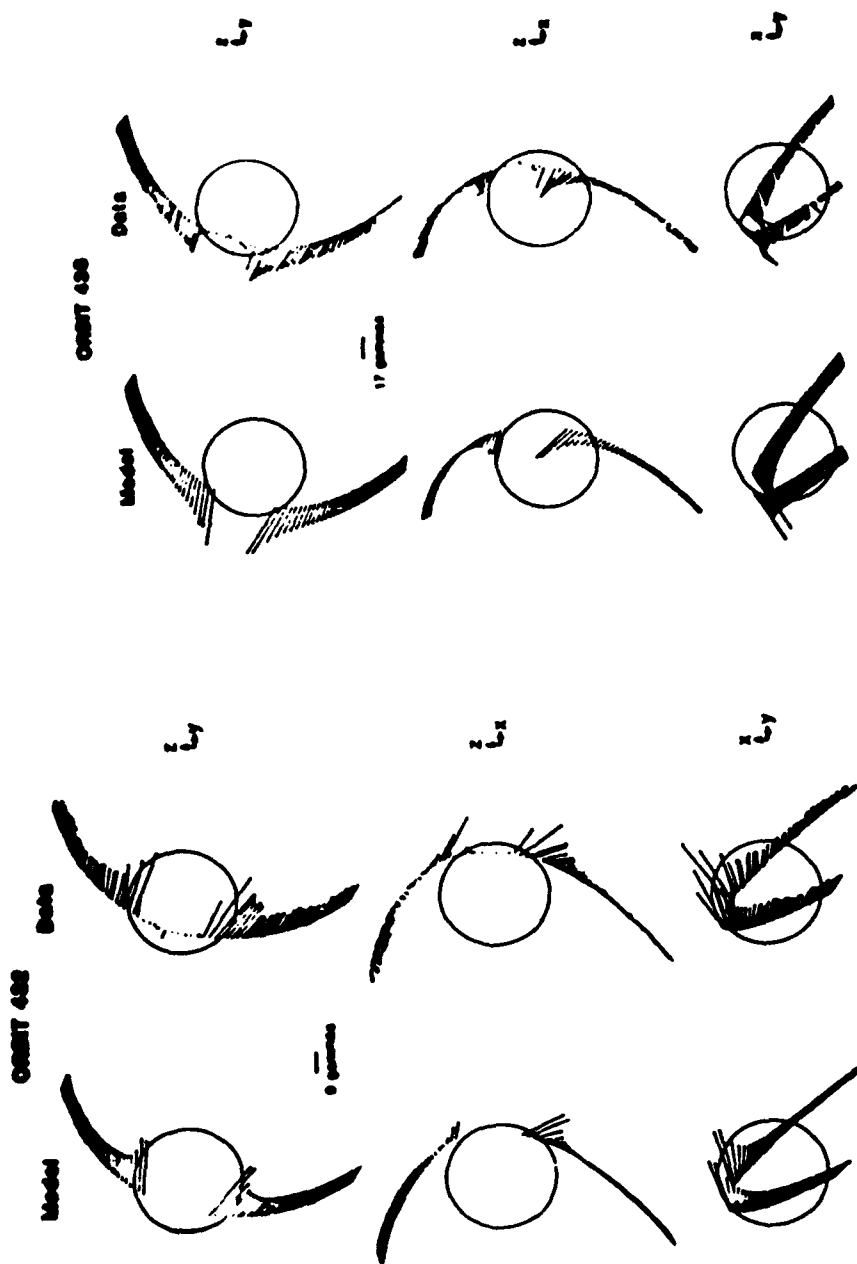


Figure 9. More Recent Validation of Elements of SUT Model: Evaluation of Convected Magnetic Field Model by Comparison With Pioneer-Venus Observations of Magnetic Field

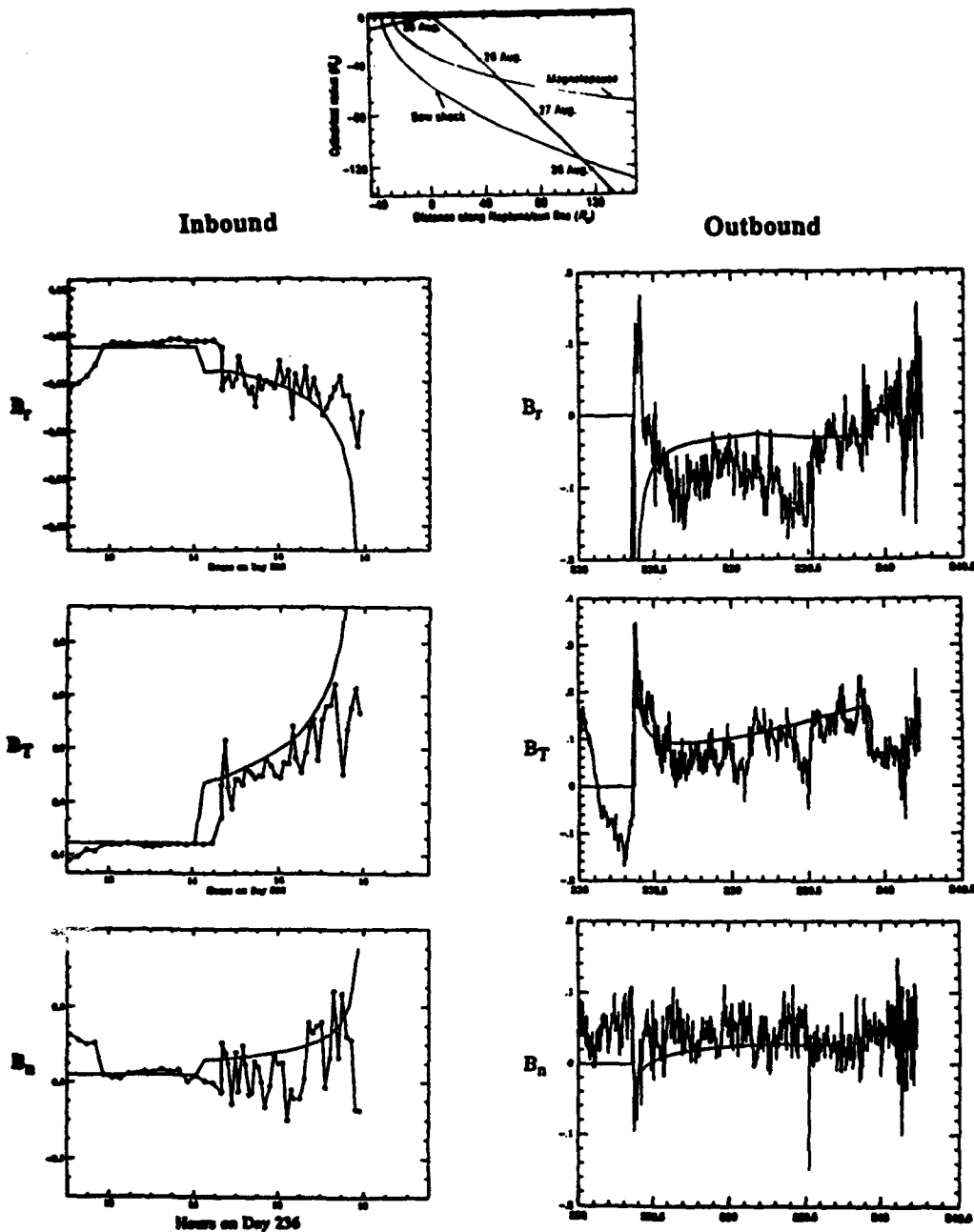
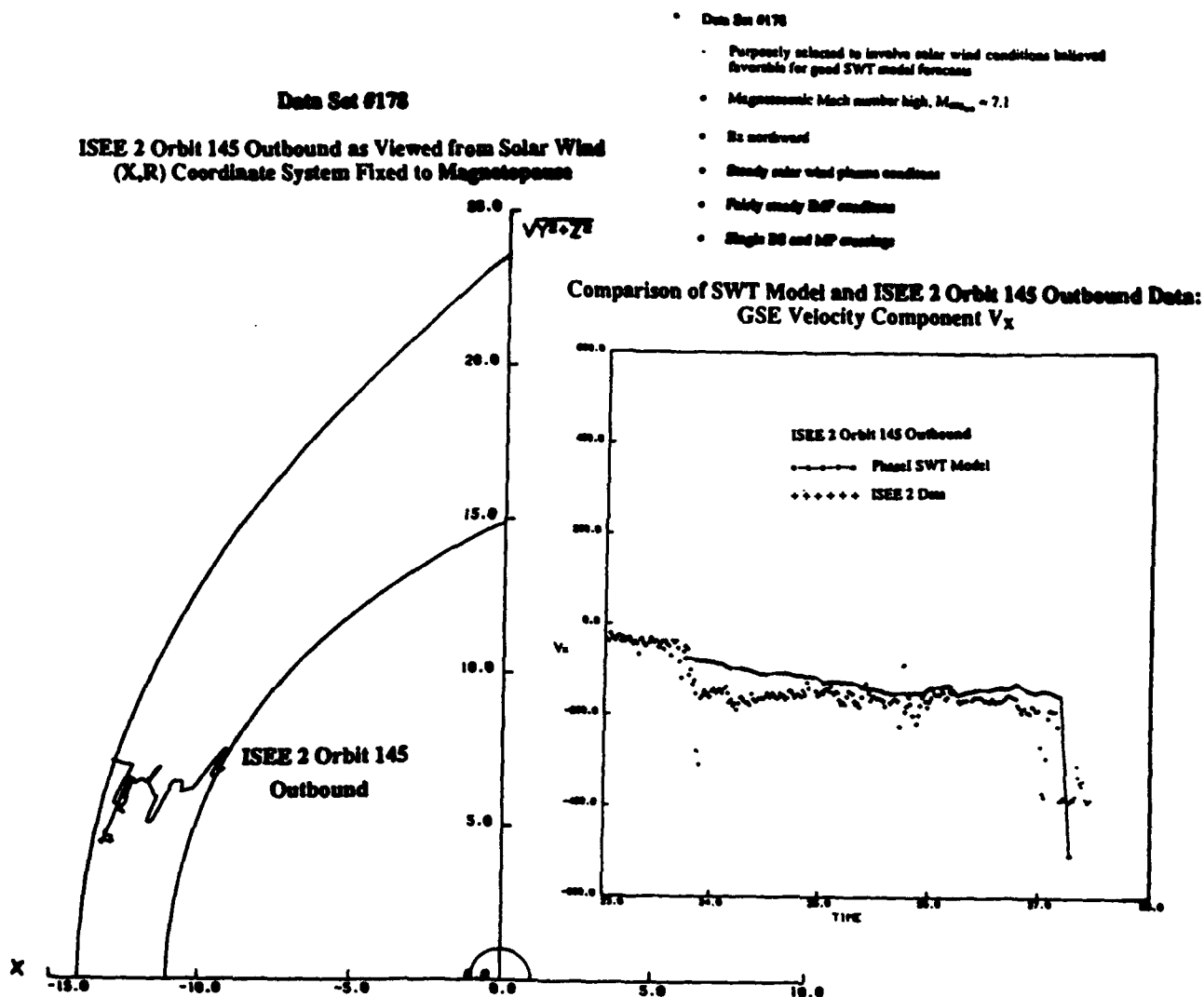
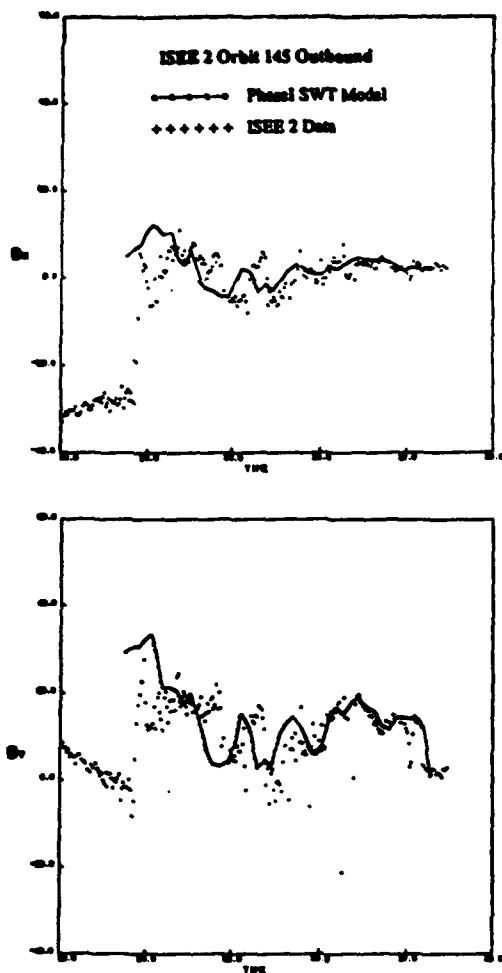


Figure 10. More Recent Validation of Elements of SWT Model: Evaluation of Convected Magnetic Field Model at Extreme Low Density Flow Situation ( $n = 0.005/\text{cm}^3$ ) by Comparison With Voyager 2 Observations at Neptune



**Figure 11. Comparison of SWT Model Forecasts and ISEE 2 Observations for Orbit 145 Outbound: ISEE 2 Orbit in Solar Wind Coordinates and Comparison of GSE Velocity Component  $V_x$**





• Data Set #178

- Purposely selected to involve solar wind conditions believed favorable for good SWT model forecasts
- Magnetosonic Mach number high,  $M_{\text{mag}} = 7.1$
- $B_z$  northward
- Steady solar wind plasma conditions
- Fairly steady IMF conditions
- Single BS and MP crossings

Figure 12. Comparison of SWT Model Forecasts and ISEE 2 Observations for Orbit 145 Outbound: GSE Magnetic Field Components

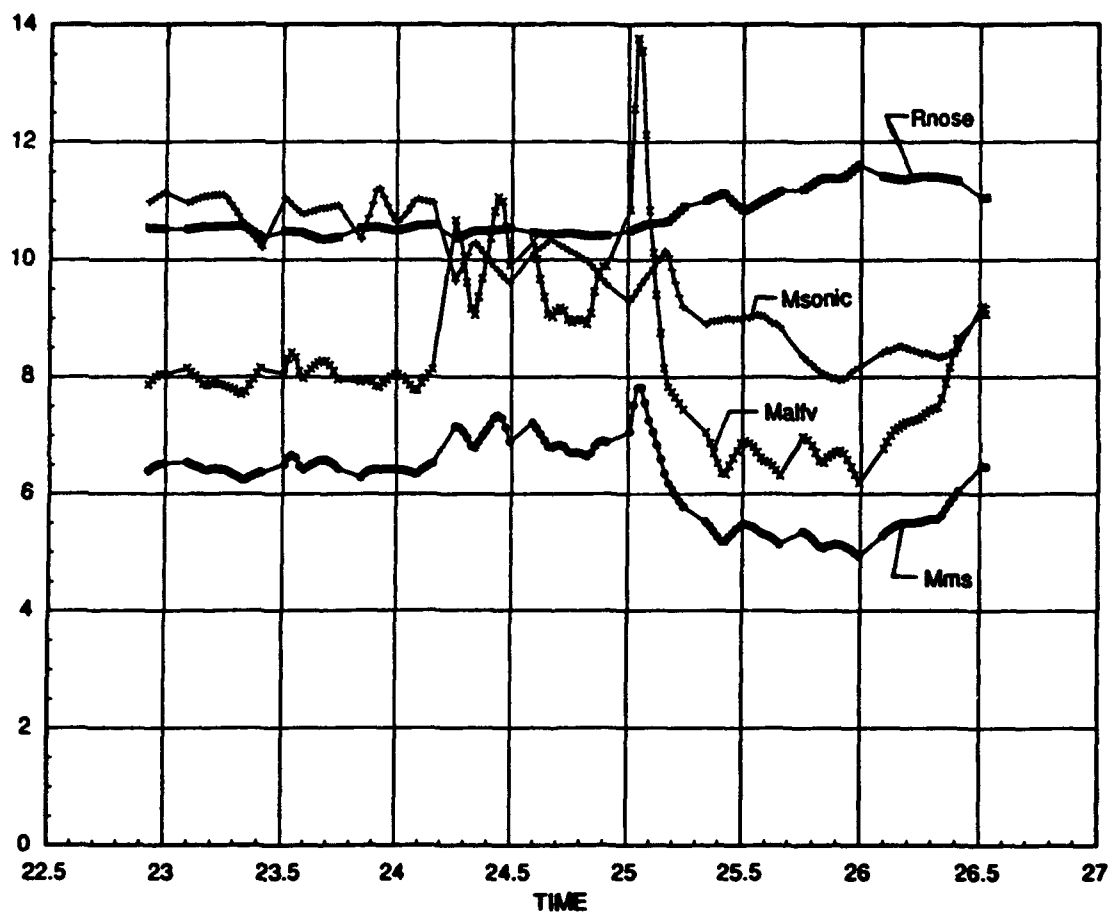


Figure 13. Illustration of Variation of Solar Wind Sonic, Alfven and Magnetosonic Mach Number and Magnetopause Nose Radius During ISEE 2 Orbit 145 Magnetosheath Traversal

# Data Set #181

ISEE 2 Orbit 178 Inbound as Viewed from Solar Wind  
(X,R) Coordinate System Fixed to Magnetopause

## Data Set #181

- Purposely selected to involve some solar wind conditions believed unfavorable for good SWT model forecasts
- Magnetosonic Mach number high,  $M_{sw} = 8.0$
- $B_z$  northward
- Moderately unstable solar wind plasma conditions
- Moderately unstable IMF conditions
- Multiple IS crossings

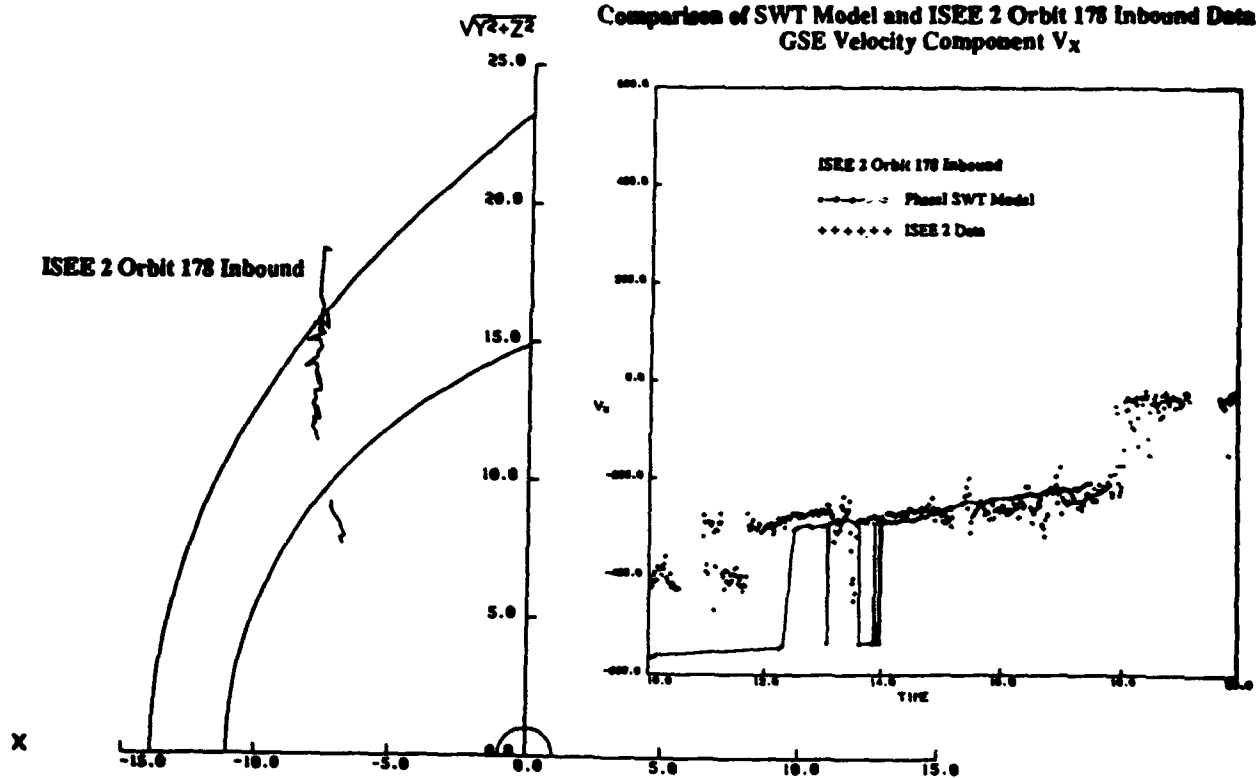
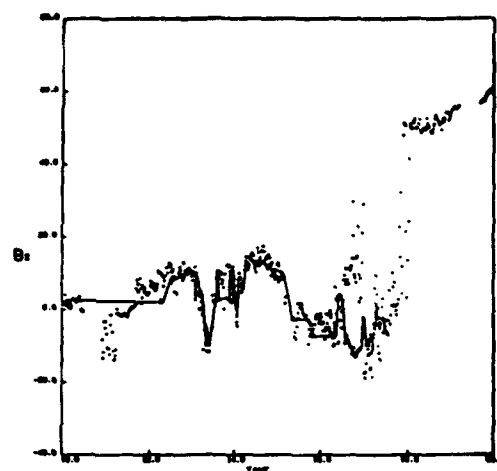
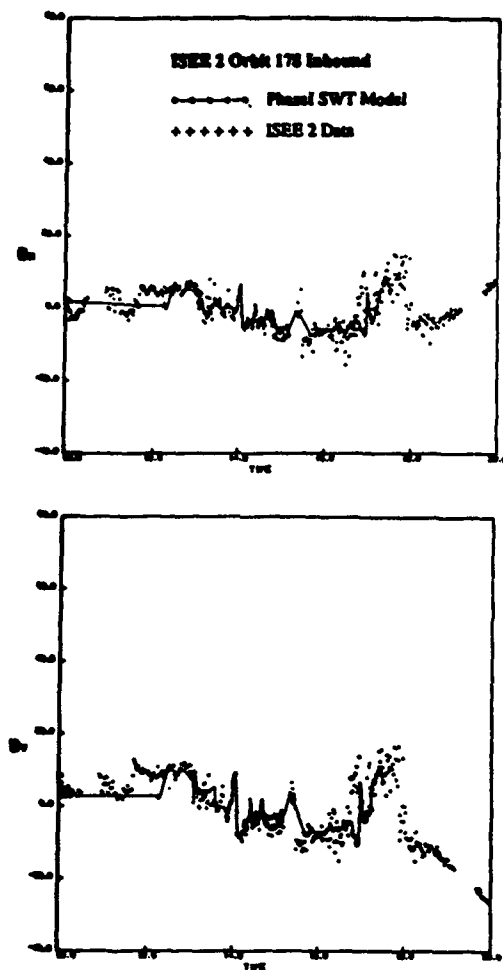


Figure 14. Comparison of SWT Model Forecasts and ISEE 2 Observations for Orbit 178 Inbound: ISEE 2 Orbit in Solar Wind Coordinates and Comparison of GSE Velocity Component  $V_x$



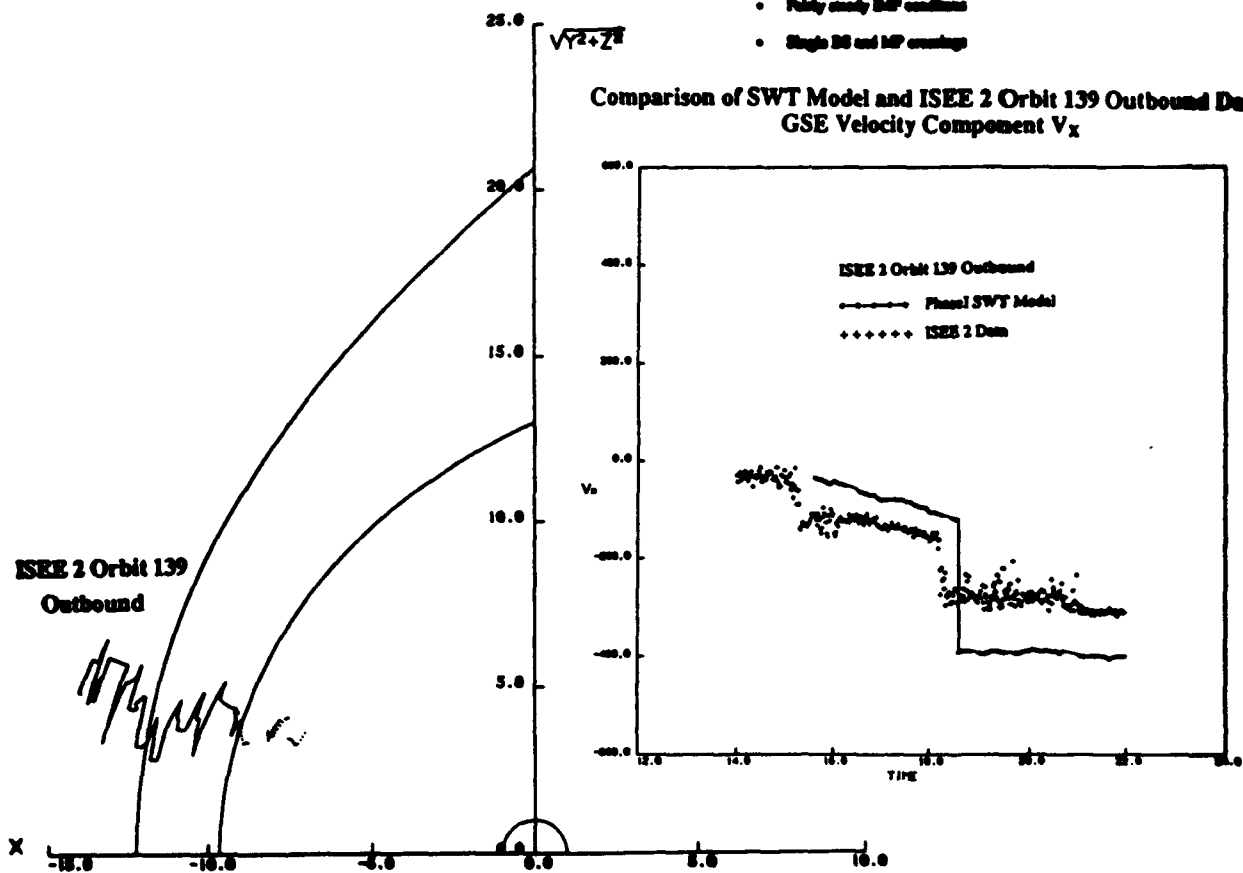
- Data Set #181
  - Purposely selected to involve some solar wind conditions believed unfavorable for good SWT model forecasts
  - Magnetosonic Mach number high,  $M_{ms} \approx 8.0$
  - $B_z$  northward
  - Moderately unsteady solar wind plasma conditions
  - Moderately unsteady IMF conditions
  - Multiple BS crossings

Figure 15. Comparison of SWT Model Forecasts and ISEE 2 Observations for Orbit 178 Inbound: GSE Magnetic Field Components

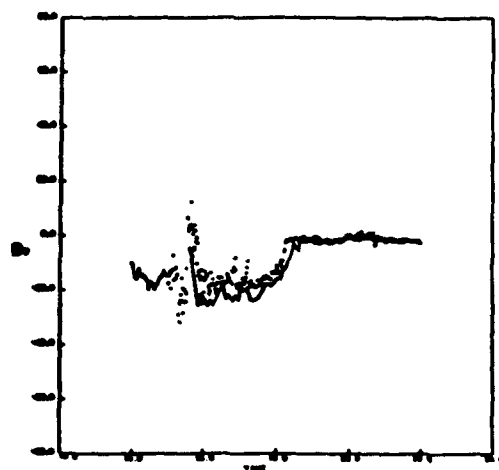
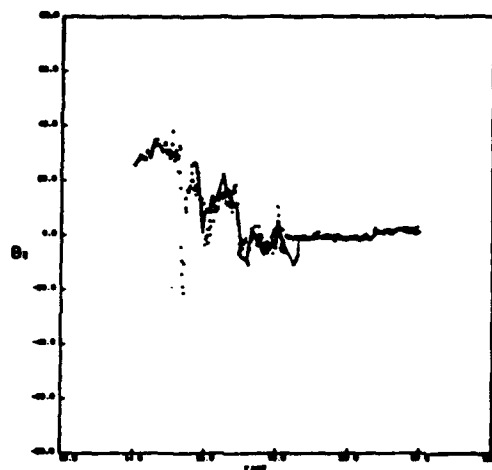
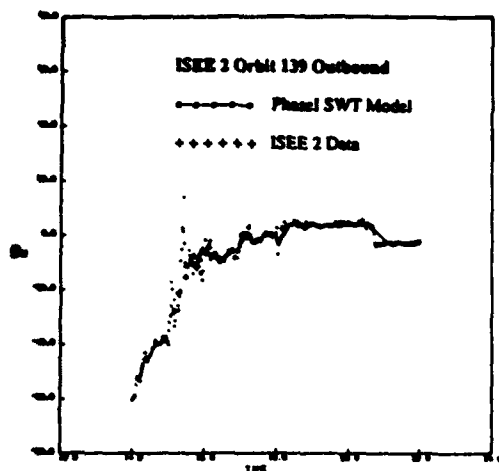
# **Data Set #145**

**ISEE 2 Orbit 139 Outbound as Viewed from Solar Wind  
(X,R) Coordinate System Fixed to Magnetopause**

- Data Set #145
- Purposely selected to involve solar wind conditions believed favorable for good SWT model forecasts
- Magnetosonic Mach number high,  $M_{sw} = 5.6$
- $B_z$  northward
- Steady solar wind plasma conditions
- Fairly steady IMF conditions
- Single DS and MP crossings



**Figure 16. Comparison of SWT Model Forecasts and ISEE 2 Observations for Orbit 139 Outbound: ISEE 2 Orbit in Solar Wind Coordinates and Comparison of GSE Velocity Component  $V_x$**



- Data Set #145
  - Purposely selected to involve solar wind conditions believed favorable for good SWT model forecasts
  - Magnetosonic Mach number high,  $M_{sw} = 5.6$
  - $B_z$  northward
  - Steady solar wind plasma conditions
  - Fairly steady IMF conditions
  - Single BS and MP crossings

Figure 17. Comparison of SWT Model Forecasts and ISEE 2 Observations for Orbit 139 Outbound: GSE Magnetic Field Components

### Data Set #009

ISEE 2 Orbit 319 Outbound as Viewed from Solar Wind  
(X,R) Coordinate System Fixed to Magnetopause

- Data Set #009
- Purposely selected to involve some solar wind conditions believed unfavorable for good SWT model forecasts
- Longest reversal interval, ~ 41 hrs.
- Magnetosonic Mach number low,  $M_{ms} \sim 3.0$
- $B_z$  southward
- Moderately unsteady solar wind plasma conditions
- Moderately unsteady IMF conditions
- No SS crossings
- Bary and sub MP crossings

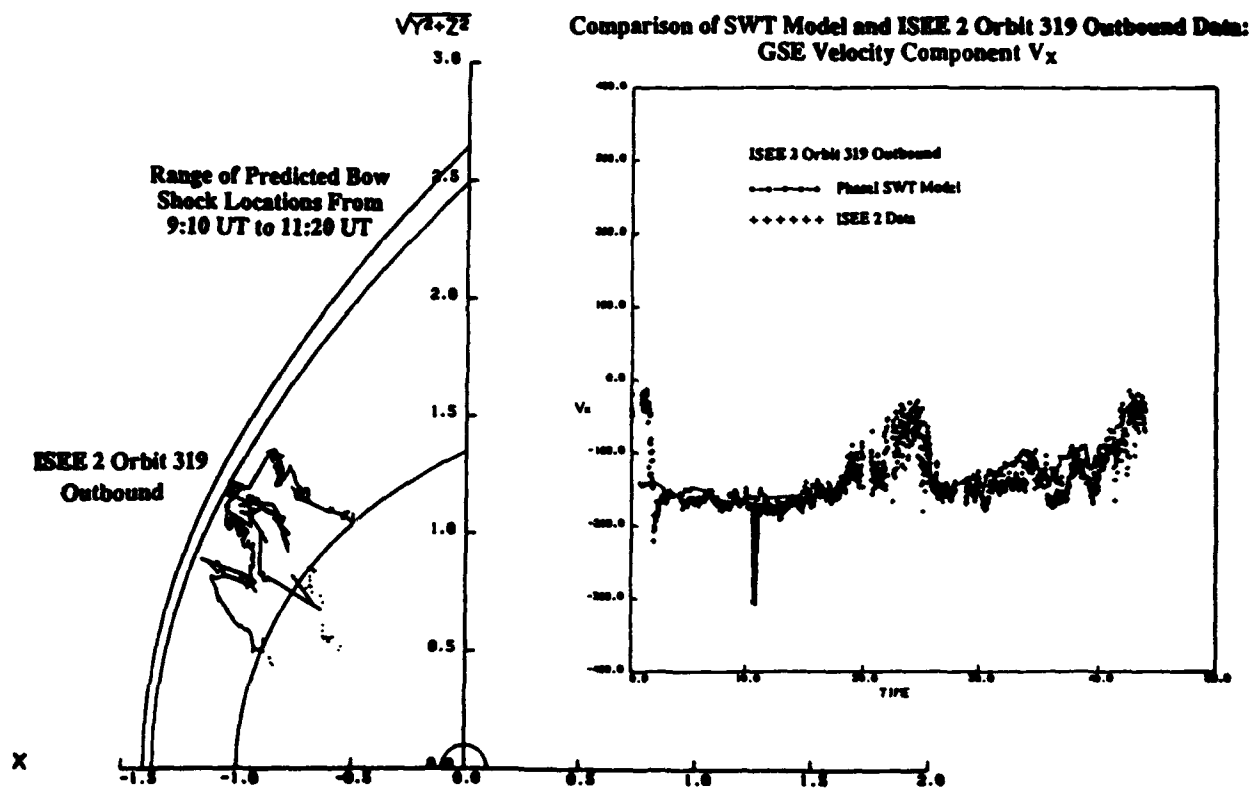
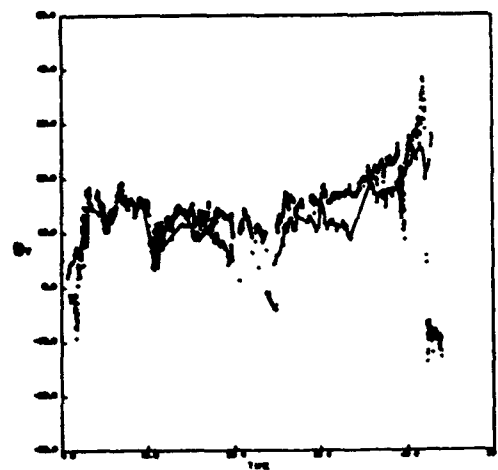
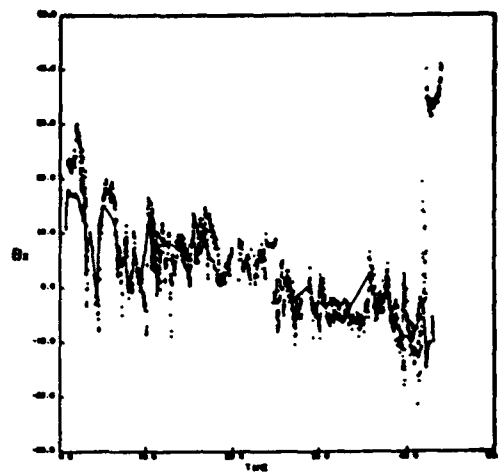
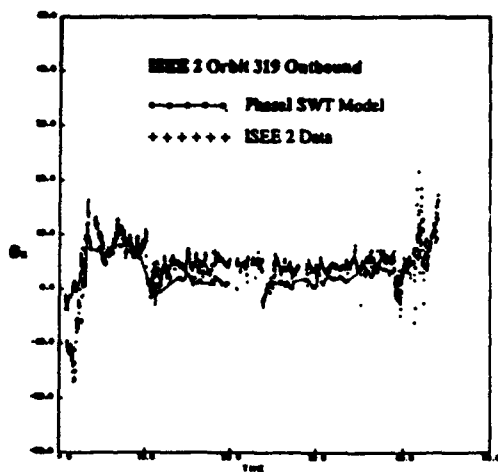


Figure 18. Comparison of SWT Model Forecasts and ISEE 2 Observations for Orbit 319 Outbound: ISEE 2 Orbit in Solar Wind Coordinates and Comparison of GSE Velocity Component  $V_x$



- Data Set #009
  - Purposely selected to involve some solar wind conditions believed unfavorable for good SWT model forecasts
  - Longest traversal interval, = 41 hrs.
  - Magnetosonic Mach number low,  $M_{ms} = 3.0$
  - Bz southward
  - Moderately unsteady solar wind plasma conditions
  - Moderately unsteady IMF conditions
  - No BS crossings
  - Entry and exit MP crossings

Figure 19. Comparison of SWT Model Forecasts and ISEE 2 Observations for Orbit 319 Outbound: GSE Magnetic Field Components



**Data Set #007**

**ISEE 2 Orbit 331 Inbound as Viewed from Solar Wind  
(X,R) Coordinate System Fixed to Magnetopause**

- Data Set #007
  - Purposely selected to involve some solar wind conditions believed unfavorable for good SWT model forecasts
  - Magnetosonic Mach number low,  $M_{ms} = 2.9$
  - Bz equatorial
  - Moderately unsteady solar wind plasma conditions
  - Moderately unsteady IMF conditions
  - Multiple BS and single MP crossings

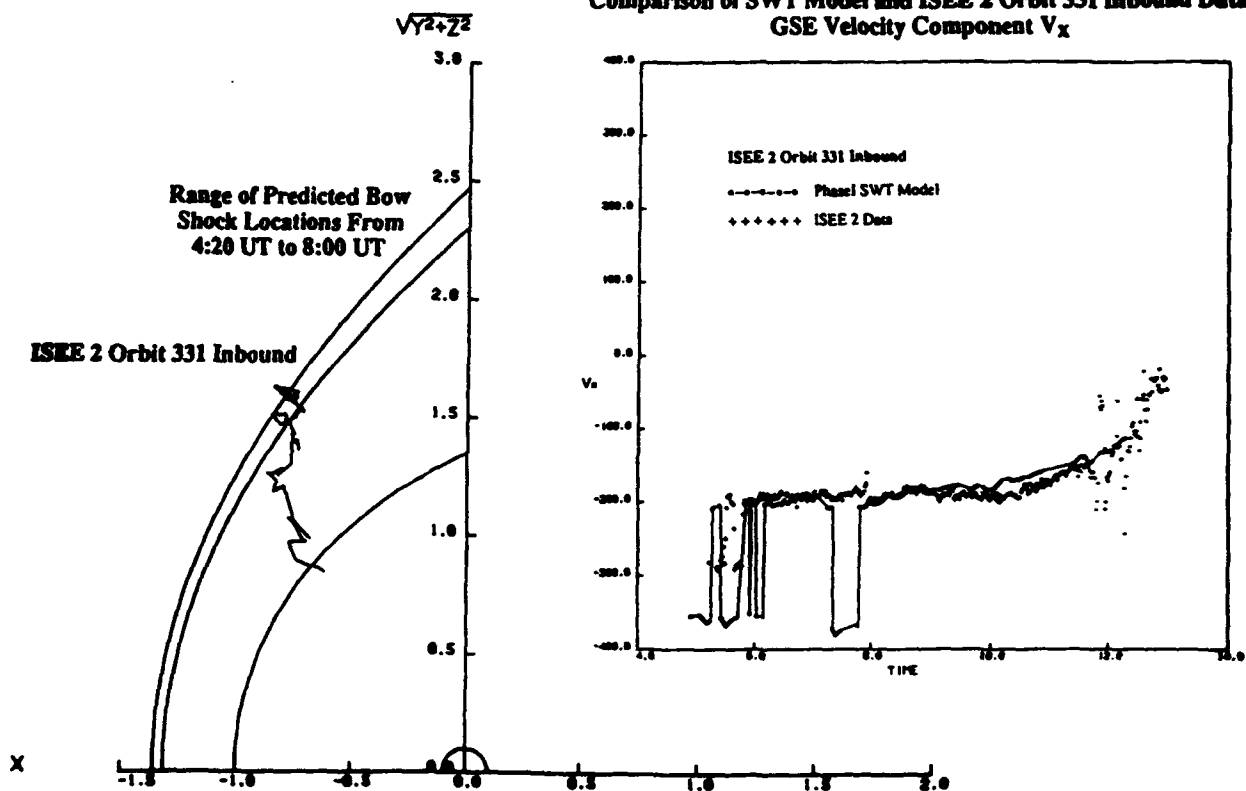
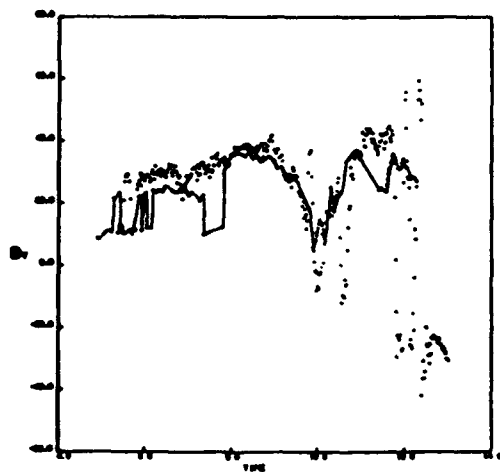
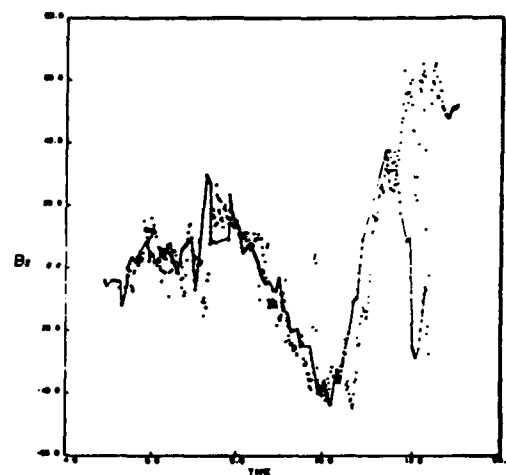
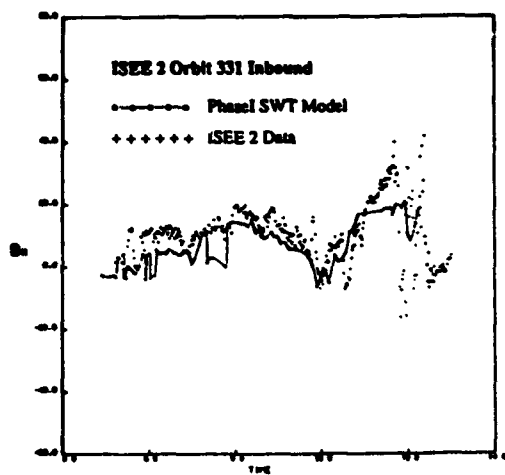


**Figure 20. Comparison of SWT Model Forecasts and ISEE 2 Observations for Orbit 331 Inbound: ISEE 2 Orbit in Solar Wind Coordinates and Comparison of GSE Velocity Component  $V_x$**



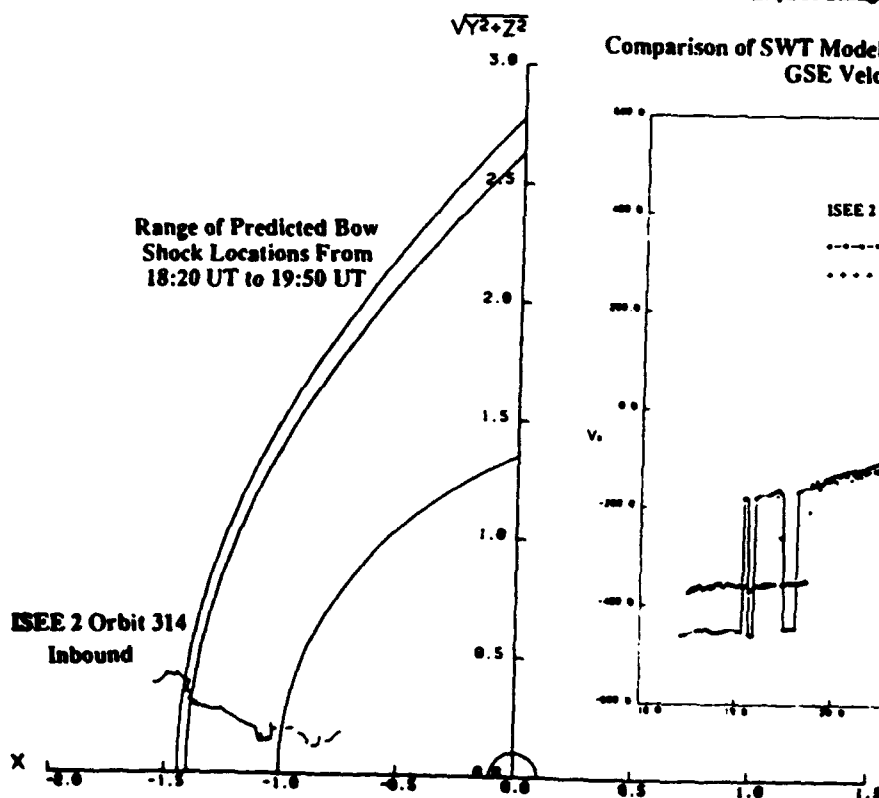
• Data Set #007

- Purposely selected to involve some solar wind conditions believed unfavorable for good SWT model forecasts
- Magnetosonic Mach number low,  $M_{ms} = 2.9$
- $B_z$  equatorial
- Moderately unsteady solar wind plasma conditions
- Moderately unsteady IMF conditions
- Multiple BS and single MP crossings

Figure 21. Comparison of SWT Model Forecasts and ISEE 2 Observations for Orbit 331 Inbound: GSE Magnetic Field Components

### Data Set #003

ISEE 2 Orbit 314 Inbound as Viewed from Solar Wind  
(X,R) Coordinate System Fixed to Magnetopause



### Data Set #3

- Purposely selected to involve some solar wind conditions believed unfavorable for good SWT model forecasts
- Magnetosonic Mach number low,  $M_{sw} = 2.2$
- Moderately unsteady solar wind plasma conditions
- Moderately unsteady IMF conditions
- Multiple BS crossings

### Comparison of SWT Model and ISEE 2 Orbit 314 Inbound Data: GSE Velocity Component $V_x$

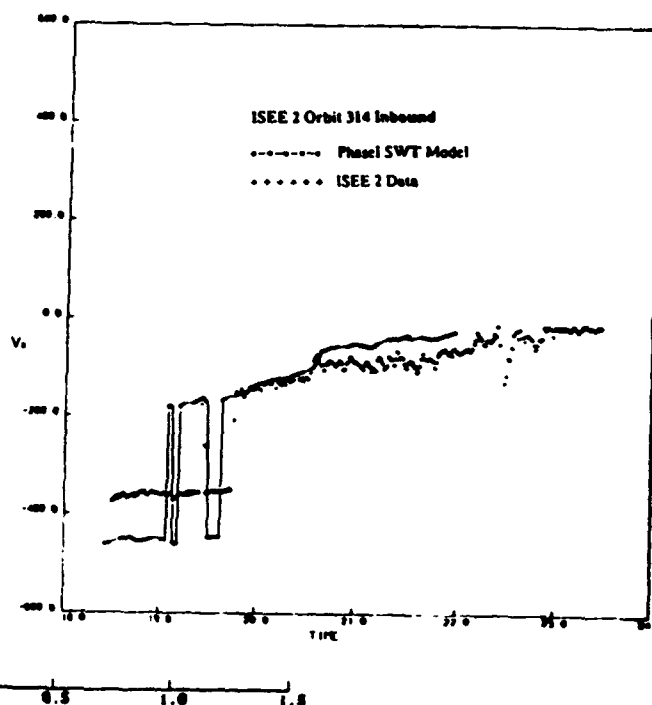
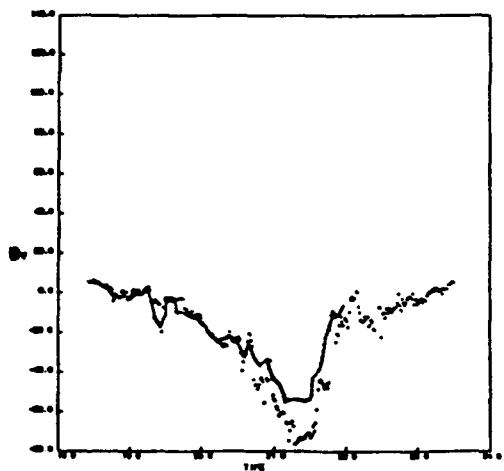
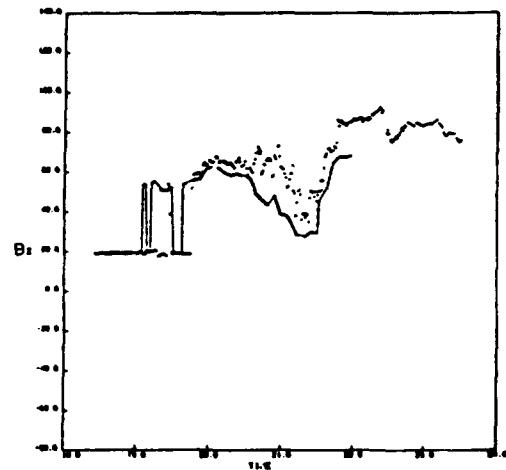
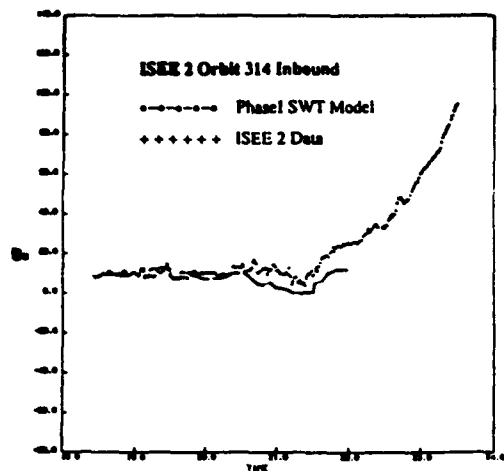


Figure 22. Comparison of SWT Model Forecasts and ISEE 2 Observations for Orbit 314 Inbound: ISEE 2 Orbit in Solar Wind Coordinates and Comparison of GSE Velocity Component  $V_x$



• Data Set #3

- Purposely selected to involve some solar wind conditions believed unfavorable for good SWT model forecasts
- Magnetosonic Mach number low,  $M_{ms} = 2.2$
- Moderately unsteady solar wind plasma conditions
- Moderately unsteady IMF conditions
- Multiple BS crossings

Figure 23. Comparison of SWT Model Forecasts and ISEE 2 Observations for Orbit 314 Inbound: GSE Magnetic Field Components